



2008

INVESTIGATING THE EFFECT OF STRESS, WETTING, AND COMPACTION ON SETTLEMENT POTENTIAL OF MINE SPOILS

Lauren M. Little

University of Kentucky, Lauren.little@uky.edu

Recommended Citation

Little, Lauren M., "INVESTIGATING THE EFFECT OF STRESS, WETTING, AND COMPACTION ON SETTLEMENT POTENTIAL OF MINE SPOILS" (2008). *University of Kentucky Master's Theses*. 525.
http://uknowledge.uky.edu/gradschool_theses/525

This Thesis is brought to you for free and open access by the Graduate School at UKnowledge. It has been accepted for inclusion in University of Kentucky Master's Theses by an authorized administrator of UKnowledge. For more information, please contact UKnowledge@sv.uky.edu.

ABSTRACT OF THESIS

INVESTIGATING THE EFFECT OF STRESS, WETTING, AND COMPACTION ON SETTLEMENT POTENTIAL OF MINE SPOILS

Strip mining in Kentucky has left large areas of land that could potentially be used for business and housing developments. However, the mine spoils underlying these areas are prone to severe differential settlement due to a variety of factors. Mine spoil from the Gateway Business Park in Jenkins, Kentucky was used for a series of laboratory tests to develop relationships between shear wave velocity, confining stress, compaction energy, and dry unit weight to develop a method to assess settlement potential. It was found that a stress-corrected shear wave velocity of greater than $275 \text{ ft/s/psi}^{0.25}$ typically indicated dry mine spoil, and less than $275 \text{ ft/s/psi}^{0.25}$ typically indicated wet mine spoil. Equations were developed to predict the amount of settlement of a mine spoil profile based on the load, the mine spoil lithology, and the shear wave velocity of the mine spoil. With regards to compaction, it was found that if the mine spoil was compacted to at least 120 pcf (18.8 kN/m^3), or a void ratio of 0.45 or less, the mine spoil would suffer little to no volume change when wetted. The results provided herein form the basis of a methodology for screening mine spoil sites for development based on settlement potential.

KEYWORDS: Mine Spoil Fill, Mine Spoil Settlement, Compaction of Mine Spoil, Hydroconsolidation, Mountaintop Removal

Lauren M. Little
05/01/2008

INVESTIGATING THE EFFECT OF STRESS, WETTING, AND COMPACTION ON
SETTLEMENT POTENTIAL OF MINE SPOILS

By

Lauren M. Little

Michael E. Kalinski, Ph.D., PE
Director of Thesis

Kamyar C. Mahboub, Ph.D.
Director of Graduate Studies

05/01/2008

THESIS

Lauren M. Little

The Graduate School
University of Kentucky

2008

INVESTIGATING THE EFFECT OF STRESS, WETTING, AND COMPACTION ON
SETTLEMENT POTENTIAL OF MINE SPOILS

THESIS

A thesis submitted in partial fulfillment of the
requirements for the degree of Masters of Science in
Civil Engineering in the College of Engineering
at the University of Kentucky

By

Lauren M. Little
Lexington, Kentucky

Director: Dr. Michael E. Kalinski, Professor of Civil Engineering
Lexington, Kentucky

2008

ACKNOWLEDGEMENTS

I would like to acknowledge the guidance, support and knowledge of my director, Dr. Michael E. Kalinski, P.E. This thesis would not have been possible without his guidance and support. Special thanks also goes to Qore Property Sciences, Inc. and Dr. Wayne Karem, PE, who contributed heavily to the research presented in this thesis.

Funding for this research was provided by the Kentucky Science and Engineering Foundation under Award # KSEF-633-RDE-007. Their support is greatly appreciated.

TABLE OF CONTENTS

Acknowledgements.....	iii
List of Tables	vi
List of Figures.....	vii
List of Files	viii
Chapter One: Introduction	1
1.1 Background.....	1
1.2 Research Objectives	3
1.3 Technical Approach.....	3
Chapter Two: Literature Review	5
2.1 Previous Research	5
2.2 Geotechnical Properties of Kentucky Mine Spoil	5
2.3 Geotechnical Properties of Reclaimed Mine Lands	8
2.4 Coalfields Regional Industrial Park Case Study.....	9
2.5 Development of a Predictive Model to Evaluate Mine Spoil Fills for Industrial Development.....	11
2.6 Summary.....	12
Chapter Three: Description of Test Materials	14
3.1 Introduction	14
3.2 Location of Samples	14
3.3 Spoil Mineralogy	15
3.4 Spoil Engineering Properties	17
3.5 Summary.....	18
Chapter Four: Effect of Confining Stress and Wetting on Settlement Potential	20
4.1 Introduction	20
4.2 Lab Procedure.....	21
4.2.1 Lab procedure for measurement of Δe of reconstituted specimens due to stress change and wetting.....	22
4.2.2 Lab procedure for estimating e_0 using v_s measurement	23
4.3 Results	24
4.3.1 Effect of confining stress on change in void ratio	25
4.3.2 Effect of wetting on change in void ratio	28
4.3.3 Estimate of e_0 using v_s measurement	30
4.4 Procedure for Estimating Settlement in Mine Spoils	34
4.4.1 Characterization of the mine spoil profile	35
4.4.2 Calculation of settlement potential	35
4.5 Summary.....	37
4.5.1 Example problem.....	38

Chapter Five: Effect of Compaction Effort and Moisture Content on Settlement Potential	41
5.1 Introduction	41
5.2 Lab Procedure.....	41
5.3 Results	45
5.3.1 <i>Effect of compaction effort on relative change in volume</i>	45
5.3.2 <i>Effect of moisture content on relative change in volume</i>	48
5.3.3 <i>Effect of dry unit weight and initial void ratio on relative change in volume</i> ...	49
5.4 Summary.....	52
Chapter Six: Summary and Recommendations	53
6.1 Research Summary	53
6.2 Future Research	55
Appendix A.....	57
References.....	59
Vita	61

LIST OF TABLES

Table 2.1, Material descriptions of tested mine spoil (Ebelhar, 1976).....	6
Table 2.2, Geotechnical properties of mine spoils (Ebelhar, 1976).....	7
Table 2.3, Compaction results for MS1, MS2, and MS3 samples (Ebelhar, 1976).....	7
Table 3.1, Summary of sample mineralogy	16
Table 3.2, Summary of mine spoil properties.....	19
Table 4.1, Regression coefficients from fitting of $e - \sigma_o'$ data to Equation 4.8.....	28
Table 4.2, Strain measurements from wetting of mine spoil specimens	29

LIST OF FIGURES

Figure 1.1, Mountaintop removal schematic (Karem et al., 2007).....	1
Figure 1.2, Illustration of valley fill construction (Skelly and Loy, 1979).....	2
Figure 2.1, Regional map showing Hazard, Kentucky, location of the Coalfields Regional Industrial Park (Karem et al., 2007).....	10
Figure 2.2, Crack in the Coalfields Regional Industrial Park office building (Karem et al., 2007)	10
Figure 3.1, Map of the Gateway Industrial Park near Jenkins, Kentucky, with the six sample recovery locations indicated (Kentucky Cabinet for Economic Development, 2005).....	15
Figure 3.2, Gradation curves of mine spoils used in this study	18
Figure 4.1, Schematic of free-free resonant column method.....	23
Figure 4.2, Photographs of typical reconstituted specimen before and immediately after wetting (view is looking down on specimen)	25
Figure 4.3, Typical relationship between e and σ_o' with stress/wetting sequence indicated (specimen from Location 6, wetted at 6.0 psi).....	26
Figure 4.4, Summary $e - \sigma_o'$ data from each test location	27
Figure 4.5, Typical auto power spectra derived from free-free resonant column testing (specimen from Location 6).....	31
Figure 4.6, Relationship between v_s' and e for each test location and specimen.....	33
Figure 4.7, Relationship between v_s' and e for all data	34
Figure 4.8, Example subsurface profile	38
Figure 5.1, Sample setup showing triaxial cell and sample close-up	42
Figure 5.2, Sample end cap and vacuum line	43
Figure 5.3, Pressure board	43
Figure 5.4, Compaction curves for soil L1/2/6 and L3/4/5.....	47
Figure 5.5, Volumetric strain versus dry unit weight	48
Figure 5.6, Volumetric strain versus moisture content.....	49
Figure 5.7, Volumetric strain versus dry unit weight	50
Figure 5.8, Volumetric strain versus initial void ratio	51

LIST OF FILES

thesis_LittleL.pdf 1.5 MB

CHAPTER 1

INTRODUCTION

1.1 Background

Mountaintop removal coal mining is a relatively inexpensive and widespread method for coal removal that is used throughout eastern Kentucky and other coal mining regions. Mountaintop removal works by stripping the overburden (soil and rock) to expose the coal seams which are then mined. The overburden that is generated, called mine spoil, is typically then dumped into adjacent valleys and then stacked to create benches. This process typically creates acres of relatively flat land (Karem, 2005). The large, flat expanses that are generated by valley fills can be used for construction of schools, housing, and light commercial development. The valley fills can have depths greater than one hundred feet. Figure 1.1 shows a schematic of how mountain removal works.

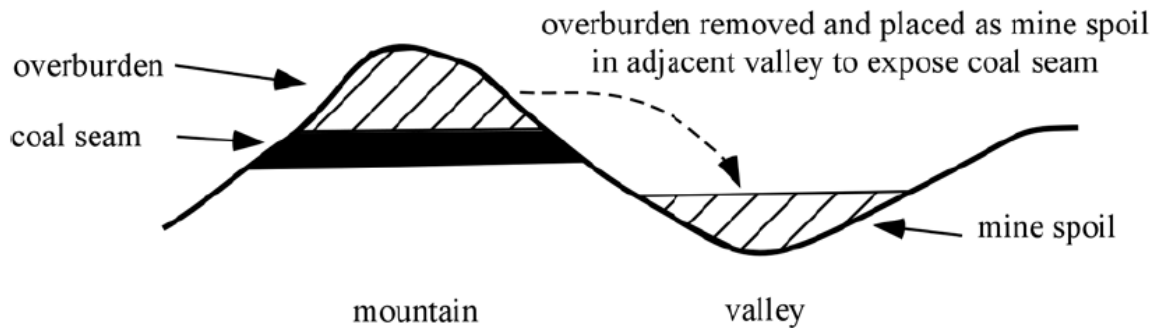


Figure 1.1. Mountaintop removal schematic (Karem et al., 2007).

Mine spoil fills are typically built using draglines or dump trucks. In the case of draglines, the dragline will sit on a bench and cast mine spoil in long continuous rows (called windrows), and eventually bulldozers will level the windrows. With this method, the mine spoil that is placed first is subject to some dynamic compaction due to additional material being placed on top of it. In the second method, dump trucks will end dump the mine spoil

into the valley and eventually scrapers or bulldozers will level it into benches (Karem, 2005). End dumping tends to create a very loose mine spoil structure that is therefore very prone to differential settlement. In addition, the variation in contouring methods (scrapers versus bulldozers) can create interfaces between areas that are susceptible to differential settlement (Karem, 2005). Figure 1.2 illustrates a typical valley fill construction.

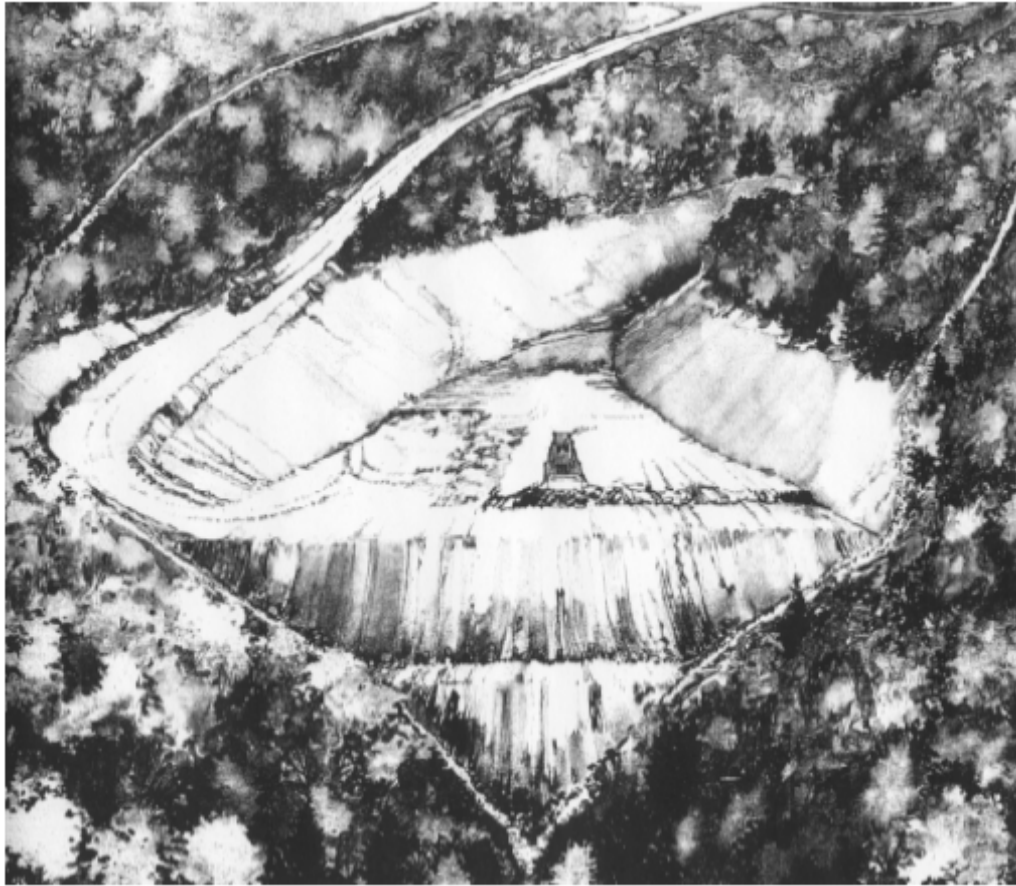


Figure 1.2. Illustration of valley fill construction (Skelly and Loy, 1979).

In addition to being placed with little to no control on compaction or fill depths, mine spoil is very heterogeneous by nature and its lithologic components tend to make it prone to differential settlement. Mine spoil in eastern Kentucky and adjacent regions is comprised heavily of shaly, silty, and angular rock fragments. These particles tend to slake when wetted and crush at inter-particle points of contact where stresses are high. In addition, the particles

are prone to stress-induced crushing, which occurs when the inter-particle stresses become large enough to crush the particles at points of contact.

There have been several case studies done on mine spoil in eastern Kentucky regarding sites that have shown large amounts of differential settlement. Two of the more notable cases include the Appalachian Regional Hospital in Hazard and the Coalfields Regional Industrial Park near Hazard. Both sites showed significant structural damage due to differential settlement of mine spoil (Karem et al., 2007). Because of the risks associated with building on these mine spoil valley fills, a better understanding of the settlement potential of these sites is needed.

1.2 Research Objectives

The objective of this research was to determine the effect of stress, wetting, and compaction on the settlement potential of mine spoil from Eastern Kentucky. A second objective was to develop a predictive model to quantify the amount of settlement that would occur under various loading conditions, as well as determine a field methodology to determine whether or not existing mine spoil had undergone hydrocompression.

1.3 Technical Approach

Mine spoil from six locations in the Gateway Business Park near Jenkins, Kentucky was used for the research reported herein. The research was performed in three stages:

- Stage 1: Measure the effects of stress and wetting on loose mine spoil.
 - This was done by placing loose mine spoil samples in a latex membrane and then confining and wetting the samples using a pressure board.
- Stage 2: Measure the shear wave velocity through the loose mine spoil specimen at varying stress and wetted states.

- Stage 3: Perform standard and modified Proctor compaction tests on the mine spoil, and then wet the Proctor specimens in a triaxial cell using a pressure board.
 - Volume change was used to quantify the settlement potential of the mine spoil for the various stress and wetted states, as well as for the compacted specimens.

CHAPTER TWO

LITERATURE REVIEW

2.1 Previous Research

Considerable research has been conducted regarding the hazards associated with building on mine spoil in recent years. The majority of the research performed in recent years has involved settlement characteristics of Eastern Kentucky mine spoil and potential predictive models for this material.

2.2 Geotechnical Properties of Kentucky Mine Spoils

Ebelhar (1976) performed several geotechnical characterization tests on mine spoil that was characteristic of the mine spoil found in Eastern Kentucky. Four manufactured blends were tested as well as two naturally occurring spoils. The test materials were obtained in Kentucky from sites in Breathitt County, Laurel County and Knox County. The manufactured spoils were made by blending four naturally occurring coal seam materials. Table 2.1 shows a summary of the materials tested.

Table 2.1. Material descriptions of tested mine spoil (Ebelhar, 1976).

Sample ID	Description	AASHTO Classification	USCS Classification
MS-G	1/3 sandstone, 1/3 siltstone, 1/3 calcareous shale blend	A-2-4	SM-SC
MS-H	1/3 sandstone, 1/3 siltstone, 1/3 acid shale blend	A-2-4	SM-SC
MS-I	1/3 sandstone, 1/3 acid shale blend, 1/3 calcareous shale blend	A-2-4	SM-SC
MS-J	1/3 siltstone, 1/3 acid shale, 1/3 calcareous shale blend	A-2-4	SC
MS1	similar to MS-J (different batch and gradation)	A-1-a(0)	GW
MS2	highwall light brown shale	A-1-a(0)	GW
MS3	gravelly sands and sandstones	A-1-b(0)	SP

Ebelhar (1976) performed Atterberg limits and compaction tests (Standard effort) in compliance with ASTM standards on the mine spoil material. Table 2.2 shows the results of these tests. For the third group of mine spoils (MS1 – MS3) compaction tests were performed at three different energies: low energy (2,500 lb-ft/ft³ [1.197 x 10⁵ J/m³]), standard proctor (AASHTO T 99-70 Method D, ASTM D698), and modified proctor (AASHTO T 180-70 Method D, ASTM D1557). The results are shown in Table 2.3.

Table 2.2. Geotechnical properties of mine spoils (Ebelhar, 1976).

Sample ID	Liquid Limit (%)	Plastic Limit (%)	Plasticity Index (%)	Optimum Moisture Content (%)	Maximum Dry Unit Weight (pcf)
MS-G	22	15	7	9.8	124.6
MS-H	22	17	5	10.3	123.5
MS-I	23	16	7	10.4	123.7
MS-J	31	22	9	12.1	120.8
MS1	26	20	6	11.9	122.2
MS2	26	21	5	10.3	128.5
MS3	22	18	4	9.2	125.2

Table 2.3. Compaction results for MS1, MS2, and MS3 samples (Ebelhar, 1976).

Sample ID	Low Energy		Standard Proctor		Modified Proctor	
	Optimum Moisture Content (%)	Maximum Dry Unit Weight (pcf)	Optimum Moisture Content (%)	Maximum Dry Unit Weight (pcf)	Optimum Moisture Content (%)	Maximum Dry Unit Weight (pcf)
MS1	15.8	111.3	11.9	122.2	7.8	130.8
MS2	14.5	119.2	10.3	128.5	7.4	136.0
MS3	13.3	114.8	9.2	125.2	7.2	131.2

The results indicate that the mine spoils in this region can be expected to have fairly low and consistent PI values, ranging in value from 4% to 9%, with an average of approximately 6%. Average values for optimum moisture content and dry density for the standard Proctor method are 10.6% and 124 pcf (19.5 kN/m³), respectively.

2.3 Geotechnical Properties of Reclaimed Mined Lands

Krebs and Zipper (1997) authored a report for the Virginia Cooperative Extension on designing foundations for housing on reclaimed mine lands. In Virginia, surface mining operations are prominent, leaving the same mine spoil valley fill topography that is seen in Eastern Kentucky. According to the report, valley fills from surface mining operations are generally deeper than 20 ft (6.1 m) and can often extend deeper than 100 ft (30.5 m) (Krebs and Zipper, 1997). These fills typically settle under their own weight for many years even with proper compaction. The settlement that the mine spoil fill undergoes consists of two basic types: creep settlement and collapse settlement. Creep settlement occurs gradually over time as a result of the settlement of loose earth materials which consolidate under their own weight and the weight of materials above. Collapse settlement, which is also known as hydroconsolidation or hydrocompression, occurs when water infiltrates the mine spoil, reducing rock strength and increasing contact crushing. The second form of settlement can occur due to rising groundwater or percolating surface water. Mine spoil that is placed dry is the most susceptible to collapse settlement and will incur less creep settlement. Conversely, material that is placed wet will likely undergo very little collapse settlement and the primary settlement mechanism will be creep. This occurs because once mine spoil has undergone initial weakening and collapse due to water infiltration; it is no longer susceptible to further water damage.

Krebs and Zipper reported that the amount of settlement generally varies directly with fill depth. For example a 100-ft (30.5-m) fill will settle twice as much as a 50-ft (15-m) fill constructed with similar materials and methods. In addition, the rate of creep settlement decreases exponentially with time, a phenomenon that holds true for all soils. Also, compaction reportedly reduces settlement. For example, if a deep fill is expected to settle 10 in. (21 cm) without compaction, it would be expected to settle about 1-2 in. (3-5 cm) with good compaction. With regard to hydroconsolidation, if the material is properly compacted, only deep fills (fills greater than 20-ft [6.1-m] deep) are expected to settle significantly. Fills less than 20-ft (6.1-m) deep that are properly compacted are not expected to hydroconsolidate. In addition, fills that are placed very wet or became saturated during construction are not expected to settle further due to hydroconsolidation.

2.4 Coalfields Regional Industrial Park Case Study

The Coalfields Regional Industrial Park is located near Hazard, Kentucky in the Appalachian mining region of Eastern Kentucky (see Figure 2.1). Karem et al. (2007) produced a paper evaluating settlement that occurred at an office building at the site. The Industrial Park area was mined using mountaintop removal methods and bulldozers were used to establish the final grade on the site. This resulted in uneven compaction and thickness of the mine spoil. The mine spoil ranged in thickness from 40 to 250 ft (12 to 76.0 m) and the groundwater table was well below the ground surface. In late 2001 a cabinet manufacturing plant was constructed on the mine spoil fill. The mine spoil was excavated from beneath the building footprint and placed back using Caterpillar 825 footed rollers with static compaction. Construction specifications were based on standard Proctor (ASTM D698) results with a maximum particle size of 12 in. (30 cm). The mine

spoil was placed in 12-in. (30-cm) lifts. Construction was substantially completed by the summer of 2002.

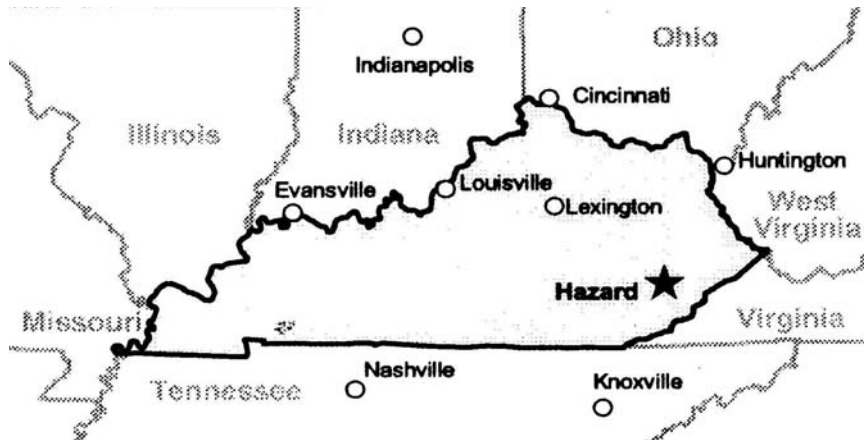


Figure 2.1. Regional map showing Hazard, Kentucky, location of the Coalfields Regional Industrial Park (Karem et al., 2007).

By March 2003 the office portion of the facility had begun to show signs of settlement. By March 2004, the northeast corner had settled approximately 4.0 in. (10 cm) and the middle of the office area had settled over 8.0 in (20 cm), relative to the original finish floor elevation. Figure 2.2 shows some of the typical damage at the site.



Figure 2.2. Crack in the Coalfields Regional Industrial Park office building (Karem et al., 2007).

Karem et al. (2007) concluded that the cause of the large differential settlement was due to hydrocompression of the recompacted mine spoil fill material. Two causes of hydrocompression were identified. First, the gutter system and additional rainwater conveyor systems were inadequate, causing overflow to drain along the building foundation. Second, portions of the site were graded to drain towards the building foundation, in particular the northwest corner. This allowed water to pool at the building foundation causing hydrocompression of the mine spoil beneath, while mine spoil that was properly drained remained stable.

Karem et al. (2007) also discussed how mine spoil that has existed in situ for many years develops an impervious “crust” of fine material that protected deeper layers from water infiltration and hydrocompression. The crust is formed from the infiltration of surface water, which leads to the piping of the fine materials. The fines eventually get lodged in the void spaces of the larger mine spoil particles creating an impervious crust. In the Coalfields case, excavating the mine spoil from beneath the building footprint destroyed the impervious crust and left the mine spoils vulnerable to future infiltration and hydrocompression.

2.5 Development of a Predictive Model to Evaluate Mine Spoil Fills for Industrial Development

Karem (2005) performed a study to develop a predictive settlement model for Eastern Kentucky mine spoil. Three mine sites were selected, the Coalfields Regional Industrial Park, the Gateway Business Park, and the Star Fire Mine. All three sites were reclaimed strip mines. The Coalfields and Gateway sites were reclaimed using end-dumping methods and the Star Fire Mine was reclaimed using draglines. All three sites were over 10 years old. Downhole extensometers and surface monuments were used at all

three sites to monitor settlement of the mine spoil. The extensometers were monitored over several years.

The study found that unsaturated mine spoil fill settles in a manner similar to clay consolidation. Initially, there is a short period of large, primary settlement, followed by a long period of secondary settlement, which is characterized by small settlements decreasing slowly with time. For end-dumped sites, surface settlements tended to be less than 2 cm (0.8 in.), while dragline sites tended to be less than 15 cm (5.9 in.). Karem (2005) also provided equations to predict settlement of mine spoil based on type of placement, age, and thickness of the mine spoil.

The study found that for most unsaturated mine spoil fills less than 100 ft thick and over 10 years old, settlement should be within allowable limits for most industrial structures. However, if the mine spoil becomes saturated, substantial structural damage due to differential settlement should be expected.

2.6 Summary

Considerable research regarding the settlement behavior and geotechnical properties of Eastern Kentucky mine spoil has been performed in recent years. The studies cited indicate that large deposits of mine spoil are very prone to differential settlement, and hydrocompression is one of the most damaging forms of settlement to occur in mine spoil. Hydrocompression is also the most prevalent cause of severe structural damage to structures placed over mine spoil deposits.

The geotechnical properties of Eastern Kentucky mine spoils tend to be fairly consistent regardless of type of spoil with regards to plasticity and compaction

characteristics. The spoils tend to be low plasticity with maximum dry unit weights ranging from 120-136 pcf (18.8-21.4 kN/m³) depending on compaction effort.

CHAPTER THREE

DESCRIPTION OF TEST MATERIALS

3.1 Introduction

All of the material used for testing was taken from six locations at the Gateway Business Park near Jenkins, Kentucky (Figure 3.1). The mine spoils taken from this site consist of mudstones, siltstones, and sandstones, and originate from mining of the Pennsylvanian coal seams. The mine spoils were the result of blasting and were placed over the area using the end dumping method by Caterpillar D10N bulldozers and 777B dump trucks. Mine spoils from the six locations were excavated and transported to the University of Kentucky (UK). At UK, the following laboratory tests were performed on the mine spoils: dry sieving (ASTM D422), specific gravity (ASTM D854), Atterberg limits (ASTM D4318), wet sieving (ASTM D1140), Unified Soil Classification System (USCS) classification (ASTM D2488), and slake durability testing (ASTM D4544). In addition, a mineralogy assessment was conducted by Warren H. Anderson of the Kentucky Geologic Survey. A full description of testing and results can be found in Rosentiel (2006).

3.2 Location of Samples

The six locations that spoils were recovered from were all within 0.75 miles (1.2 km) of each other at the Gateway Business Park (see Figure 3.1). The spoils were recovered from depths of 4.0-8.0 ft. (1.2-2.4 m) below the ground surface using a backhoe. The material was placed into 5-gallon (0.2 m³) plastic buckets and taken back to the UK geotechnical lab. Larger boulders (dimensions up to 3 ft. (0.9 m) were excluded due to the bucket size, but smaller boulders and cobbles (dimensions less than 7.9 in. (20

cm)) were brought back to the lab. It was estimated that the excluded boulders comprised approximately 30% of the total excavated material.

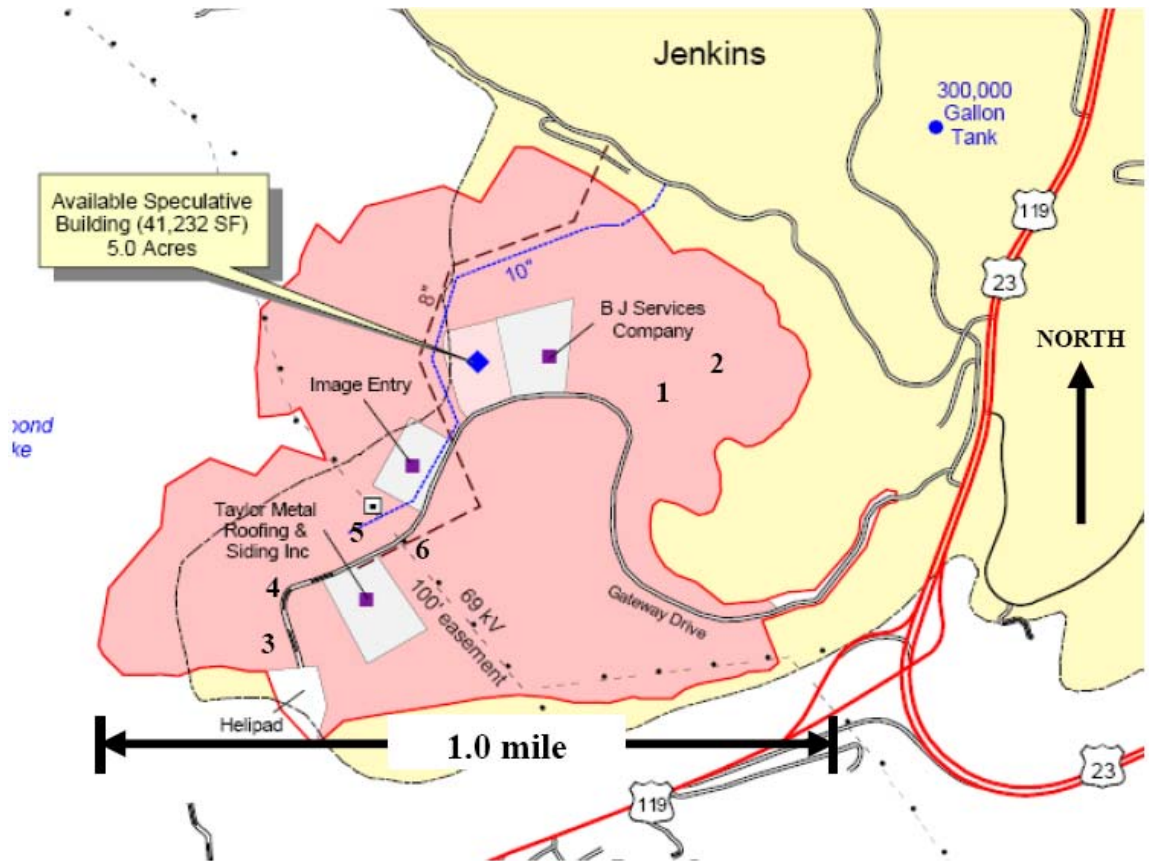


Figure 3.1. Map of the Gateway Industrial Park near Jenkins, Kentucky, with the six sample recovery locations indicated (Kentucky Cabinet for Economic Development, 2005).

3.3 Spoil Mineralogy

The six mine spoil samples underwent a complete petrological and mineralogical assessment. The assessment was conducted by Warren H. Anderson of the Kentucky Geological Survey. The samples consisted primarily of siltstones, sandstones, and mudstones and the mineralogical descriptions of each sample location are detailed in Table 3.1. It was indicated that prior to being mined, the material consisted of Pennsylvanian sandstones, siltstones, mudstones, and shales, with minor amounts of

limestone. The results also indicated that coal and most of the Amubrgy unit, or UE #3 unit, was mined in this area. Only traces of these materials existed in the samples or were a lithologic component of the original rock units that these samples originated from.

Table 3.1. Summary of sample mineralogy.

Sample ID	Mineralogical Description
L1	Siltstone, very micaceous, greenish gray, in part sandy, with clasts of feldspar and abundant coal debris; in part micaceous clay or mudstone, in part with carbonate cement, abundant mica and some iron staining.
L2	Siltstone and mudstone, very micaceous, greenish gray, in part sandy, with carbonate cement, black coal particles and debris, iron stained.
L3	Sandstone, in part micaceous, brownish yellow, abundant sand grains are frosted, both angular and spherical, in part micaceous siltstone.
L4	Sandstone, white, partly micaceous, with some coal fragments and gray micaceous siltstone.
L5	Sandstone, white to yellow, in part with coal debris.
L6	Mudstone, shaly, with some siltstone, dark gray, micaceous, with abundant coal fragments.

X-ray diffraction was also performed on two of the sample locations to determine the mineralogy. To perform the x-ray diffraction, the soil was first prepared by separating the original sample into four fractions: material passing the 0.5-in. (12.7-mm) sieve (composite fraction), material retained by the No. 4 (4.75-mm) sieve (coarse fraction), material retained by the No. 200 (0.075-mm) sieve (medium fraction), and material passing the No. 200 (0.075-mm) sieve (fine fraction). The coarse and medium fractions were washed on a No. 200 (0.075-mm) sieve to remove any fine particles that may have been attached and then the material was dried in an oven at 230°F (110°C) for 12 hours.

The segregated material was then sent to Mr. Anderson at the Kentucky Geological Survey to perform x-ray diffraction analysis of the material. Due to time constraints only Location 1 and Location 4 had x-ray diffraction performed, and Location 4 only had its composite fraction analyzed.

The results of the x-ray diffraction showed little variation in mineralogical composition between the two sample locations. The major minerals identified included vermiculite, illite, biotite, kaolinite, muscovite, and quartz. The presence of illite may explain why the material is unstable when wet. Illite has relatively little shear strength and does not support load bearing structures well as a result. The results of the four fractions from Location 1 showed little variation in the chemical structure of the sample from each of the four fractions (coarse, medium, fine, composite), which indicates that all fractions are representative of the material and that as the material breaks into finer fractions the chemical composition remains unchanged.

3.4 Spoil Engineering Properties

At the lab the spoils were oven dried and then filtered on a 0.50-in. (12.7-mm) sieve. The selection of the 0.50-in. (12.7-mm) sieve was due to the restriction that for resonant column testing the maximum grain size to specimen diameter ratio must be less than 1:6 in accordance with ASTM D4015. The specimen diameter was 4.00-in. (102-mm), requiring the maximum particle size to be 0.50 in. (12.7 mm) Dry sieve analysis (ASTM D422) was performed on all of the material that was transported to the lab (including the material greater than 0.50 in. (12.7 mm)). However, the gradation curves did not include the large boulders encountered in the field. Since it was estimated that 70% of the total material in the field was small enough to fit in the buckets, the percent

passing on the gradation curves shown in Figure 3.2 should be multiplied by 0.70 to get an overall adjusted field gradation curve that includes the larger boulders. Figure 3.2 shows the gradation curves for the six locations.

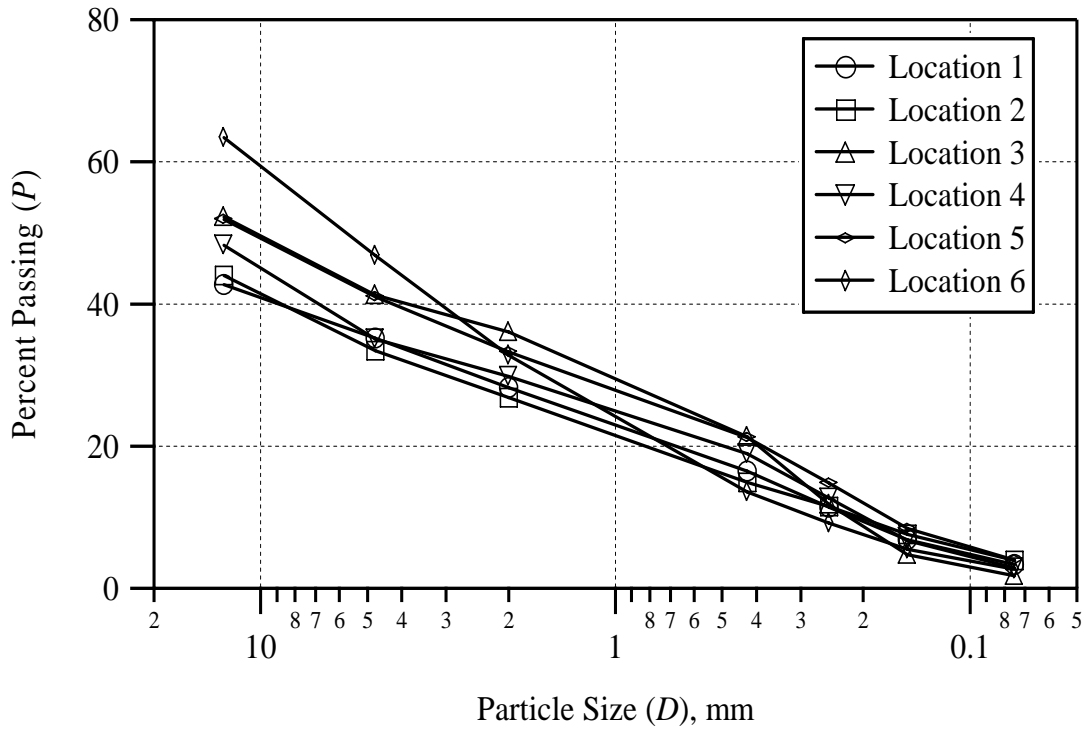


Figure 3.2. Gradation curves of mine spoils used in this study.

In addition to sieve analysis, specific gravity, Atterberg limits, wet sieving, and Unified Soil Classification (USCS), and slake durability testing was performed, the results of which are summarized in Table 3.3.

3.5 Summary

The results of the material classification testing performed on the mine spoil shows the material to be primarily well- to poorly-graded gravel with some silt, sand, and clay. The minerals present are primarily vermiculite, illite, biotite, kaolinite, muscovite, and quartz. The mine spoil locations can also be differentiated based on petrology, with

Locations 1 and 2 being primarily sandstone, Locations 3, 4, and 5 being primarily siltstone, and Location 6 being primarily mudstone.

Table 3.2. Summary of mine spoil properties.

Location	Mineralogical Description	Recovery Depth (ft)	In Situ w (%)	G_s	LL (%)	PI (%)	USCS Classification	Slake Durability Index (%)	Percent Fines by Wet Sieving
1	Siltstone	4	5.3	2.72	24.2	5.7	GC	92.1	34.7
2	Siltstone	5	5.4	2.68	26.2	4.6	GP-GC	95.8	24.1
3	Sandstone	8	7.5	2.64	22.3	0.1	GP-GM	72.4	20.6
4	Sandstone	6	5.3	2.62	21.9	--	GM	97.1	34.7
5	Sandstone	5	4.0	2.68	22.0	1.0	GM	97.1	24.1
6	Mudstone	5	7.0	2.68	26.9	5.7	GC	89.6	20.6

CHAPTER FOUR
EFFECT OF CONFINING STRESS AND WETTING ON SETTLEMENT
POTENTIAL

4.1 Introduction

Mine spoil undergoes two primary forms of settlement: stress-induced crushing and hydrocompression (Karem et al., 2007). Stress-induced crushing occurs when the inter-particle stresses become large enough to crush the particles at points of contact. In dry conditions this is the primary cause of settlement in mine spoil. However, when water is present, hydrocompression can occur, leading to substantial settlement (volume change due to contraction). Hydrocompression is an issue if the mine spoil rock fragments are silty, shaly, and angular, which is typical of Eastern Kentucky mine spoil. The rock fragments will slake when wetted and crush at the inter-particle points of contact. Once mine spoil has undergone hydrocompression it is not likely to undergo any further significant settlement. Settlement of mine spoil can be described in terms of a reduction in void ratio, Δe , due to the two primary mechanisms, stress-induced crushing and hydrocompression:

$$\Delta e = \Delta e_s + \Delta e_h, \quad (4.1)$$

where Δe_s and Δe_h are changes in void ratio due to stress-induced crushing and hydrocompression, respectively. Total settlement (S) of a layer of initial height, H_0 , is given as:

$$S = H_0 \frac{\Delta e}{1 + e_0}, \quad (4.2)$$

where e_0 is the initial void ratio of the mine spoil prior to volume change. Herein, Δe is negative when the soil decreases in volume.

To accurately predict the amount of settlement a mine spoil site is likely to undergo, the initial void ratio, e_0 , and the expected change in void ratio, Δe , due to stress-induced crushing and hydrocompression must be known. The research presented herein attempted to determine these factors by reconstituting a series of laboratory specimens to measure and quantify the effect of confining stress and wetting on Δe , and by performing shear wave velocity, v_s , measurements to develop a relationship between v_s and e for estimating e_0 . Shear wave velocity can be correlated to e using a generic relationship (e.g. Hardin and Drnevich, 1972; Seed et al., 1986):

$$v_s = f(e)(\sigma'_o)^{0.25}, \quad (4.3)$$

where σ'_o is the mean effective confining stress and $f(e)$ is a soil-specific void ratio function. As a general rule, v_s increases with increasing mean effective confining stress and decreases with increasing void ratio. As a result, v_s can be measured at a mine spoil site and correlated to e_0 using an expression similar to Equation 4.3, Δe can be predicted based on anticipated changes in σ'_o and wetting at the site. The total predicted settlement, S , can then be estimated and sites can be screened for development based on settlement potential.

4.2 Lab Procedure

The material used for this research was first oven-dried and then reconstituted into 8.00-in. (20.3-cm) long, 4.00-in. (10.2-cm) diameter specimens. The material used in the specimens was comprised of material passing the 0.50 in. (12.7 mm) sieve. Because the resonant column testing was to be performed using 4.00-in. (10.2-cm) diameter

specimens, the material coarser than the 0.50-in. (12.7-mm) sieve was excluded to maintain a maximum grain size:specimen diameter ratio less than 1:6 in accordance with the ASTM D4015 standard for resonant column testing. The materials were reconstituted in a latex membrane, which was placed in an aluminum mold to maintain a cylindrical shape. The material was placed by dry pluviation from a height of approximately 1.0 in. (2.5 cm) and efforts were made to distribute the material in a way that would minimize segregation. After the material was placed in the membrane, PVC end caps were placed on each end of the membrane and the membrane was sealed to the end caps using O-rings. A pore vacuum of 3.0 psi (21 kPa) was applied to maintain the specimen's right cylindrical shape. Three specimens were reconstituted from each sample location.

4.2.1 Lab Procedure for Measurement of Δe of Reconstituted Specimens Due to Stress Change and Wetting

The specimens were prepared according to the procedure outlined in Section 4.2, with three specimens reconstituted from each sample location. The pore vacuum was increased incrementally from 3.0 psi (21 kPa) to 6.0 psi (41 kPa) to 9.0 psi (62 kPa). Specimen volume was measured at each increment by measuring the average length and diameter of the specimen, and e was calculated at each vacuum level to measure the effect of mean effective confining stress (σ'_o , equal to the pore vacuum) on Δe_s due to stress-induced crushing.

Tap water was permeated through the dry specimens to measure the effect of wetting. Again, three specimens for each location were prepared, and each specimen was wetted at a vacuum of 3.0 psi (21 kPa), 6.0 psi (41 kPa), or 9.0 psi (62 kPa). Specimens were wetted by permeating tap water using a pressure board at a low (between 5 and 10)

hydraulic gradient. The low hydraulic gradient was used to minimize the piping within the samples. Also, the samples were not completely saturated to prevent clogging of the effluent vacuum line due to piping. The average moisture content of the specimens after wetting, w_{avg} , was approximately 13% with a corresponding average degree of saturation, S_{avg} , of approximately 66%. Specimen volume was measured, and e was calculated to measure the effect of wetting on Δe_h due to hydrocompression.

4.2.2 Lab Procedure for Estimating e_0 Using v_s Measurement

Free-free resonant column testing was performed at the end of each vacuum/wetting stage for each specimen to measure shear wave velocity, v_s , for correlation with initial void ratio, e_0 , in the specimens. The free-free resonant column method (Kalinski and Thummaluru, 2005) involves the suspension of a right circular cylindrical specimen of material as depicted in Figure 4.1.

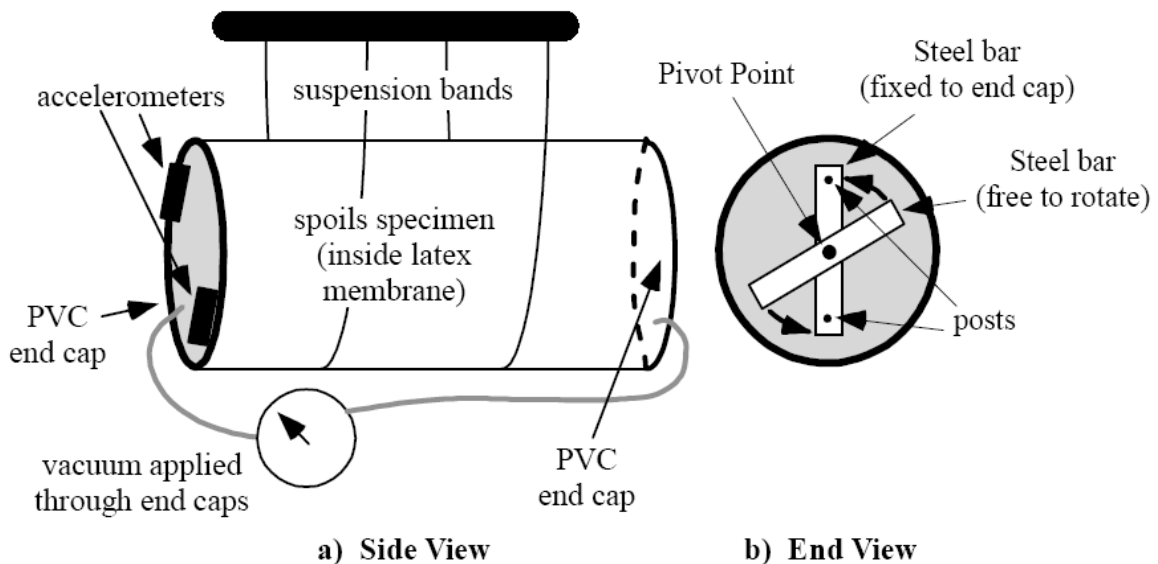


Figure 4.1. Schematic of free-free resonant column method.

The specimen is excited at one end using a transient torsional pulse, and torsional motion is measured at the other end using two accelerometers. The specimen resonates at a

torsional resonant frequency of f_n , which is derived by performing spectral analysis of the time-domain accelerometer output signal. Shear wave velocity is calculated using the following equation:

$$\beta = \frac{2\pi f_n L}{v_s} \quad (4.4)$$

where L is the specimen length and β is calculated using the following relationship:

$$\tan \beta = \frac{(\mu_1 + \mu_2)\beta}{\mu_1\mu_2\beta - 1} \quad (4.5)$$

For Equation 4.5,

$$\mu_1 = \frac{I_1}{I} \quad (4.6)$$

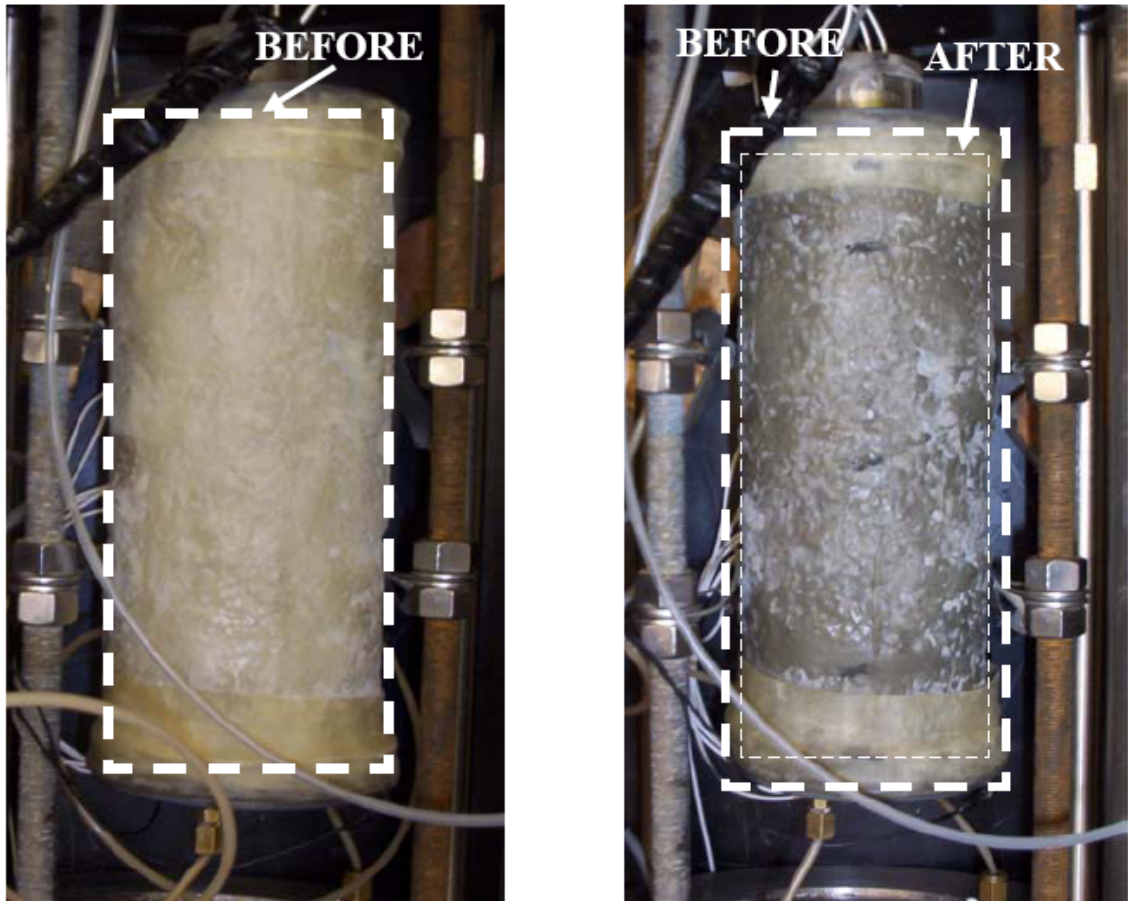
and

$$\mu_2 = \frac{I_2}{I}, \quad (4.7)$$

where I_1 and I_2 are the polar mass moments of inertia of the masses fixed to each end of the specimen, and I is the polar mass moment of inertia of the specimen. After v_s was calculated for each vacuum and wetting stage, the data were analyzed to establish a relationship between v_s and e_0 .

4.3 Results

The samples that were wetted showed almost immediate volume reduction. Typical results from measurement of a single sample are illustrated in Figure 4.2.



(a) Before wetting

(b) After wetting

Figure 4.2. Photographs of typical reconstituted specimen before and immediately after wetting (view is looking down on specimen). Note the decrease in specimen area indicated by the dashed white rectangles.

4.3.1 Effect of confining stress on change in void ratio

Typical results for a sample are illustrated in Figure 4.3. Figure 4.3 shows that reduction in e due to confining stress (stress-induced crushing) is relatively small compared to the reduction in e due to wetting (hydrocompression).

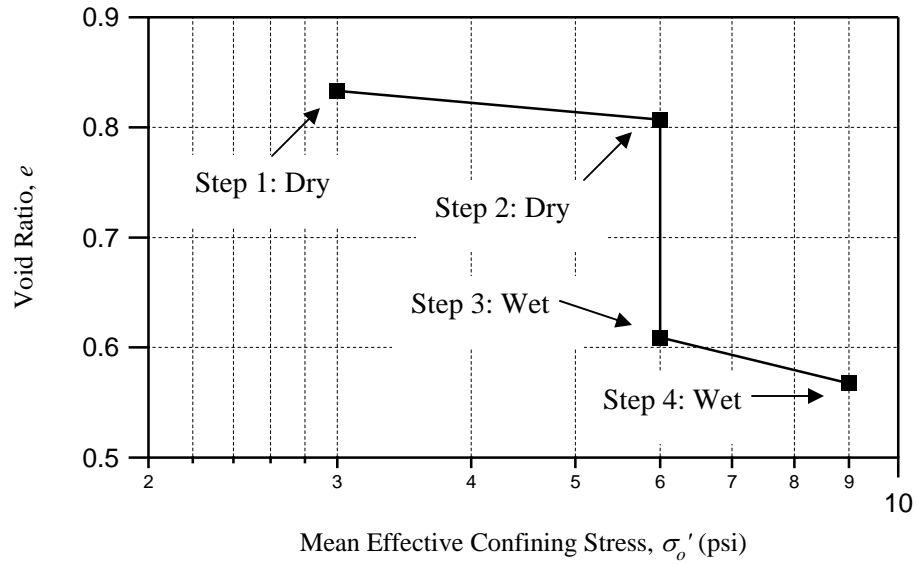


Figure 4.3. Typical relationship between e and σ'_o with stress/wetting sequence indicated (specimen from Location 6, wetted at 6.0 psi).

To quantify the effects of stress-induced crushing on Δe , the $e - \sigma'_o$ data were plotted for each location and is shown in Figure 4.4.

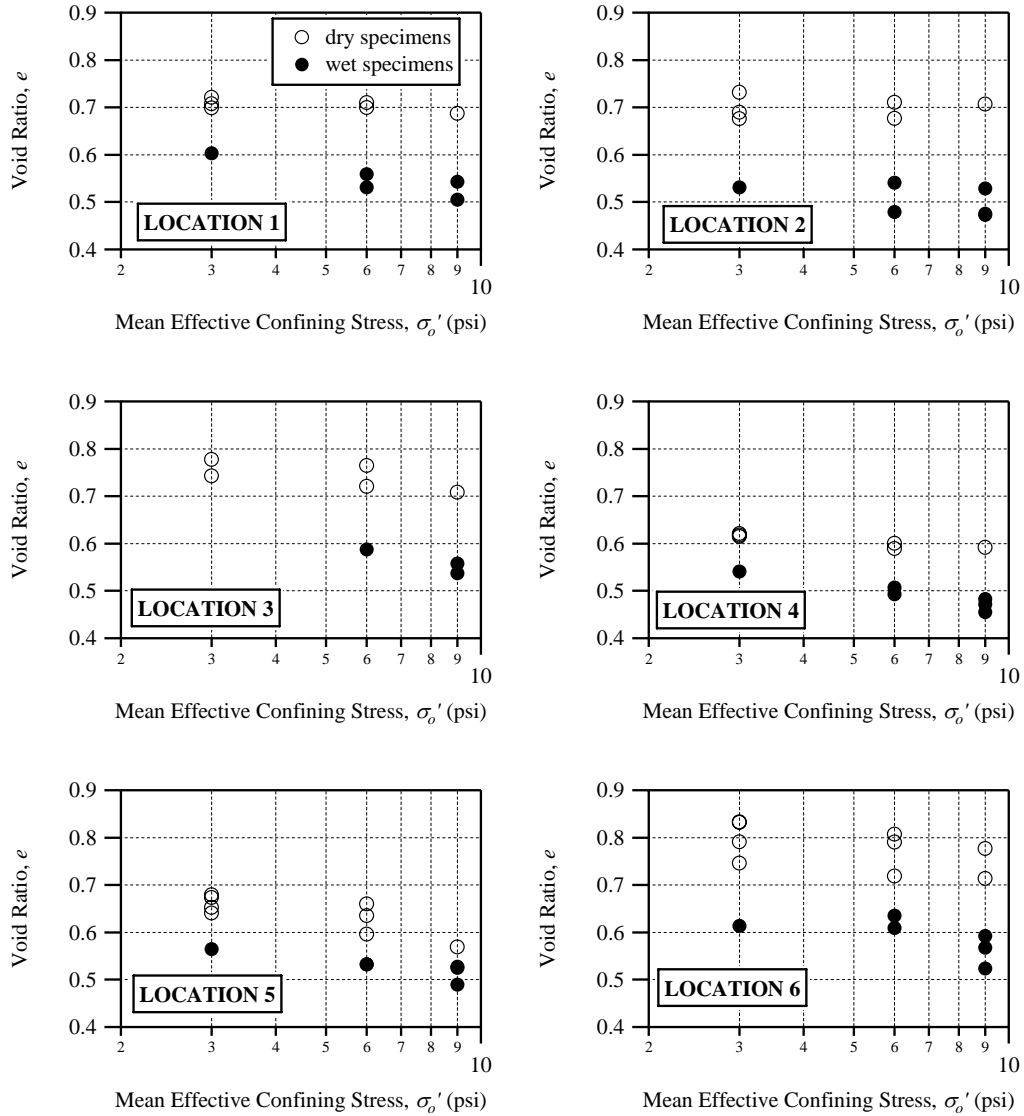


Figure 4.4. Summary $e - \sigma'_0$ data from each test location.

Using regression analysis, the data shown in Figure 4.4 were fitted to the relationship:

$$e = C_s[\log(\sigma'_0)] + b, \quad (4.8)$$

where C_s and b are regression coefficients. The regression coefficient, C_s , can be defined as the stress-induced crushing index, which ultimately can be used to estimate the settlement due to stress-induced crushing of the mine spoil, S_s ;

$$S_s = \frac{H_0}{1 + e_0} C_s \log\left(\frac{\sigma'_f}{\sigma'_i}\right), \quad (4.9)$$

where σ'_i and σ'_f are the in situ vertical effect stresses before and after loading, respectively.

Table 4.1 shows the results of the regression analysis, which indicate that spoils that have been wetted are susceptible to larger amounts of stress-induced crushing settlement than dry spoils due to a higher C_s coefficient in wetted spoils. The higher C_s value for wet spoils is due to the fact that mine spoil becomes weak when wetted and is crushed more easily at the inter-particle contact points. The average value of C_s for dry specimens is 0.075 and the average for wet specimens is 0.142.

Table 4.1. Regression coefficients from fitting of $e - \sigma'_o$ data to Equation 4.8.

Lithology	Location	Dry Specimens			Wet Specimens		
		C_s	b	Chi-Squared (X^2)	C_s	b	X^2
siltstones	1	-0.035	0.727	0.00040	-0.164	0.677	0.00120
	2	+0.005	0.695	0.00234	-0.083	0.573	0.00392
sandstones	3	-0.094	0.808	0.00178	-0.225	0.762	0.00021
	4	-0.062	0.646	0.00013	-0.151	0.615	0.00052
	5	-0.154	0.738	0.00400	-0.105	0.615	0.00087
mudstones	6	-0.111	0.854	0.01160	-0.127	0.694	0.00499
Averages		-0.075	0.745	0.00338	-0.142	0.656	0.00195

4.3.2 Effect of wetting on change in void ratio

The results of change in e due to wetting (hydrocompression) are summarized on Table 4.2. For each sample, the void ratios before and after wetting (e_0 and e_f , respectively) are shown. Average values for e_0 and e_f are 0.68 and 0.54, respectively. The average strain for all specimens was around 10%.

Table 4.2. Strain measurements from wetting of mine spoil specimens.

Lithology	Location	Wetting Stress (psi)	e before wetting, e_i	e after wetting, e_f	Δe	Strain, ε	Average Strain, ε_{avg}
siltstones	1	3	0.70	0.60	0.10	0.06	0.08
	1	6	0.71	0.56	0.15	0.09	
	2	3	0.68	0.53	0.14	0.09	
	2	6	0.68	0.54	0.14	0.08	
	2	9	0.71	0.53	0.18	0.10	
sandstones	3	6	0.76	0.59	0.18	0.10	0.07
	3	9	0.71	0.54	0.17	0.10	
	4	3	0.62	0.54	0.08	0.05	
	4	6	0.59	0.49	0.10	0.06	
	4	9	0.59	0.48	0.11	0.07	
	5	3	0.68	0.56	0.11	0.07	
	5	6	0.64	0.53	0.10	0.06	
5	9	0.57	0.49	0.08	0.05		
mudstones	6	3	0.79	0.61	0.18	0.10	0.11
	6	6	0.81	0.61	0.20	0.11	
	6	9	0.71	0.52	0.19	0.11	

The change in void ratio due to hydrocompression, Δe_h , is also included in Table 4.2 and is expressed as:

$$\Delta e_h = e_0 - e_f \quad (4.10)$$

Strain for each specimen due to wetting, ε , is expressed as:

$$\varepsilon = \frac{\Delta e_h}{1 + e_0} \quad (4.11)$$

Strain ranges from 0.05 to 0.11 and correlates to the sample lithology (i.e. mudstones tend to be more susceptible to settlement due to hydrocompression and sandstones tend to be less susceptible). In addition, samples with a more clayey mineralogy (i.e. siltstones and mudstones) tended to have the highest average strain values. This is due to the fact that clays tend to have large reductions in internal shear strength when they become wet,

which makes it difficult for the individual clay particles to retain their shape in the presence of confining stress. Using the strain value, settlement due to hydrocompression, S_h , can be expressed as:

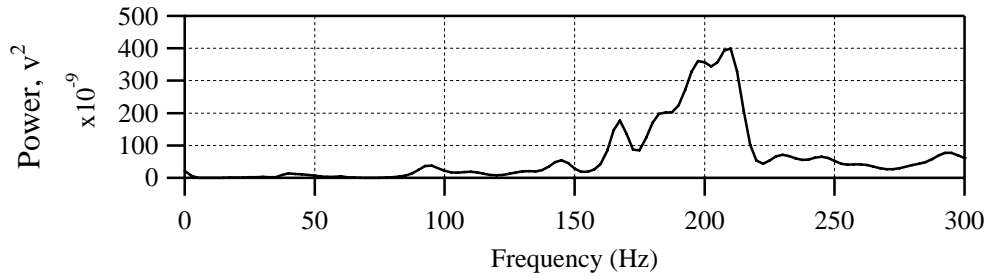
$$S_h = H_0 \varepsilon, \quad (4.12)$$

and total settlement caused by stress-induced crushing and hydrocompression can be calculated by combining Equations 4.9 and 4.12, giving:

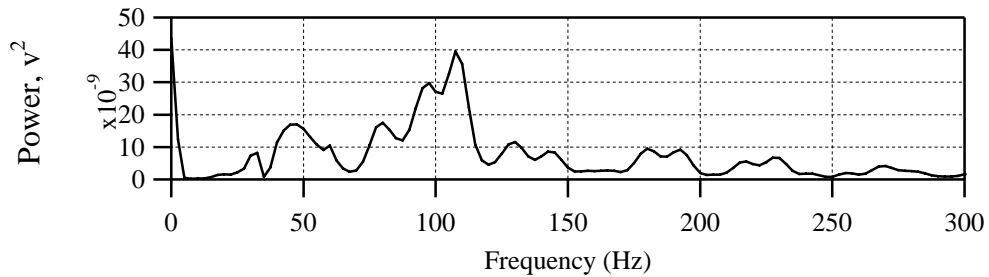
$$S = S_s + S_h. \quad (4.13)$$

4.3.3 Estimate of e_0 using v_s measurement

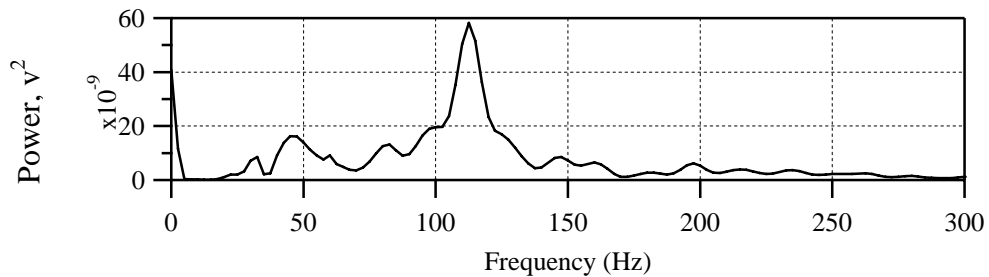
As mentioned previously, the shear wave velocity of the mine spoil samples was calculated by performing free-free resonant column testing. A series of auto power spectra generated by the free-free resonant column test for a typical specimen are shown in Figure 4.5.



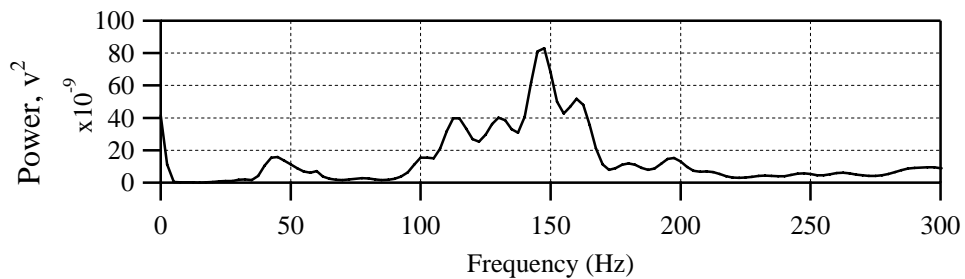
a) $\sigma'_o = 3.0$ psi, dry ($f_n = 210.0$ Hz)



b) $\sigma'_o = 3.0$ psi, wet ($f_n = 107.5$ Hz)



c) $\sigma'_o = 6.0$ psi, wet ($f_n = 112.5$ Hz)



d) $\sigma'_o = 9.0$ psi, wet ($f_n = 147.5$ Hz)

Figure 4.5. Typical auto power spectra derived from free-free resonant column testing (specimen from Location 6).

It should also be noted that shear wave velocity increases with increasing effective confining stress, σ'_o . This behavior is typical for most soils (e.g. Hardin & Drnevich,

1972). A relationship between v_s and e was developed based on the results, however v_s was first normalized with respect to the quarter root of σ'_0 to develop a stress-corrected shear wave velocity, v_s' , given as:

$$v_s' = \frac{v_s}{(\sigma'_0)^{0.25}}. \quad (4.14)$$

This stress-corrected shear wave velocity generated a shear wave velocity that was only a function of void ratio (see Equation 4.3). Figure 4.6 shows the results of the shear wave testing. In general, shear wave velocity decreases when the material is wetted. This is likely due to the softening of the crushed rock particles, as material that is softer, such as soil, generally has a lower shear wave velocity than hard materials such as rock.

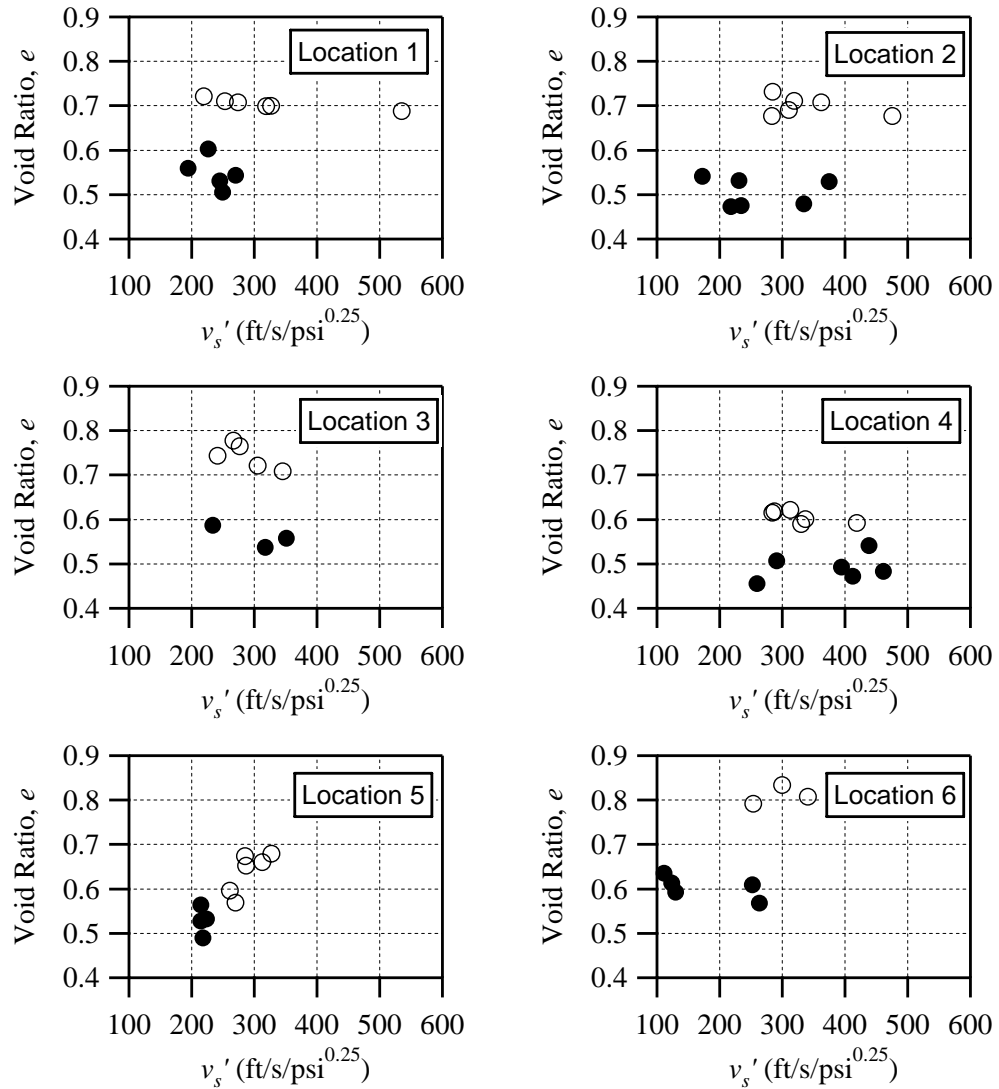


Figure 4.6. Relationship between v_s' and e for each test location and specimen.

There is a large amount of statistical variation in the results shown in Figure 4.6, likely due to the heterogeneous nature of the mine spoil. Because of this large statistical variation, a consistent relationship between v_s' and e cannot be conclusively established; therefore the data cannot be fitted to Equation 4.3. In addition, Equation 4.3 is based on the assumption that v_s is independent of σ'_o , which does not hold true for mine spoils due to stress-induced crushing. Therefore a probabilistic approach was employed to estimate

e based on v_s' . Figure 4.7 illustrates the relationship between v_s' and e for all six locations.

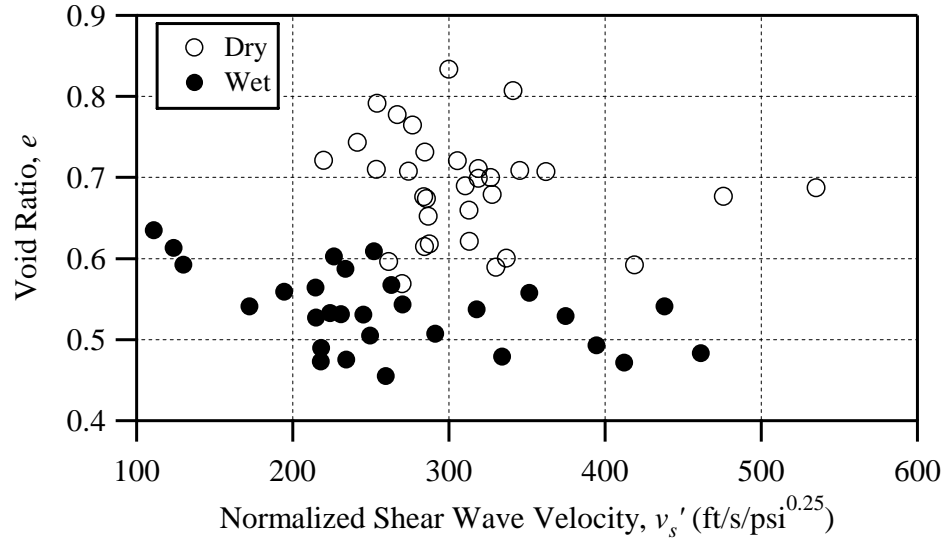


Figure 4.7. Relationship between v_s' and e for all data.

Evaluating Figure 4.7, it is apparent that when v_s' is less than $275 \text{ ft/s/psi}^{0.25}$ ($51.8 \text{ m/s/kPa}^{0.25}$), 67% of the specimens are wet. Conversely, when v_s' is greater than $275 \text{ ft/s/psi}^{0.25}$ ($51.8 \text{ m/s/kPa}^{0.25}$), 72% of the specimens are dry. For practical applications, this means that v_s measurements taken in the field and normalized with respect to in situ mean effective confining stress less than $275 \text{ ft/s/psi}^{0.25}$ ($51.8 \text{ m/s/kPa}^{0.25}$), are probably representative of mine spoil that is wet.

4.4 Procedure for Estimating Settlement in Mine Spoils

With the results from this chapter, a simple procedure has been generated to rank potential construction sites based on settlement potential. The procedure requires two primary steps and is described in the following paragraphs.

4.4.1 Characterization of the mine spoil profile

The first step for estimating settlement potential of mine spoils is to perform in situ v_s testing using a nonintrusive geophysical method such as surface waves or refraction seismic to measure variations in v_s with depth, thereby defining the mine spoil profile. A nonintrusive method is recommended due to the presence of large boulders in mine spoils, which makes drilling difficult and costly. For each interval in the profile, calculate v_s' using Equation 4.14. The mean effective confining stress can be expressed as a function of vertical effective stress (σ'_v) and the coefficient of earth pressure at rest (K_0):

$$\sigma'_o = \sigma'_v \left(\frac{1 + 2K_0}{3} \right). \quad (4.15)$$

K_0 for coarse grained, normally consolidated soil can be estimated using (Das, 2002):

$$K_0 = 1 - \sin\phi', \quad (4.16)$$

where ϕ' is the drained (or effective) friction angle of the soil.

If v_s' calculated using Equations 4.14, 4.15, and 4.16 is less than $275 \text{ ft/s/psi}^{0.25}$ ($51.8 \text{ m/s/kPa}^{0.25}$), the material is probably wet. If $v_s' > 275 \text{ ft/s/psi}^{0.25}$ ($51.8 \text{ m/s/kPa}^{0.25}$), the material is probably dry.

4.4.2 Calculation of settlement potential

After the mine spoil profile has been characterized using geophysical methods, the settlement can then be calculated. For each layer, total settlement (S) can be expressed as a weighted sum of settlement of wetted material (S_w) and dry material (S_d). Even if the mine spoil is dry, a wetted settlement value must be calculated to account for possible water infiltration or varying groundwater table during the life of the mine spoil. The

expression for S_w is derived by substituting values for e_0 and C_s of 0.54 and 0.142, respectively, in Equation 4.9:

$$S_w = 0.0922H_o \log\left(\frac{\sigma_f'}{\sigma_i'}\right). \quad (4.17)$$

The expression for S_d is derived by substituting values for e_0 and C_s of 0.68 and 0.075, respectively, into Equation 4.9, and combining Equations 4.9 and 4.12:

$$S_d = H_o \left[0.0446 \log\left(\frac{\sigma_f'}{\sigma_i'}\right) + \varepsilon \right]. \quad (4.18)$$

For Equation 4.18, ε is 0.07, 0.08, or 0.11 for mine spoil lithology of sandstone, siltstone, or mudstone respectively, and comes from the average values in Table 2. For layers within the profile that are probably wet ($v_s' < 275 \text{ ft/s/psi}^{0.25}$), S is expressed as:

$$S = 0.67S_w + 0.33S_d. \quad (4.19)$$

For layers within the profile that are probably dry ($v_s' > 275 \text{ ft/s/psi}^{0.25}$), S is expressed as:

$$S = 0.28S_w + 0.72S_d. \quad (4.20)$$

In Equations 4.17 and 4.18, H_o represents the interval over which settlement can reasonably be expected. For stress-induced settlement, this interval is limited by the depth because σ_f'/σ_i' approaches unity with increasing depth. For hydrocompression-induced settlement, this interval is limited by the interval over which wetting of dry spoils may be expected and it may be necessary to separate Equation 4.18 into components for stress-induced and hydrocompression-induced settlement using different values of H_o for each component.

Dry spoils can be wetted by two mechanisms: rising of the groundwater table and downward permeation of surface water. In the case of a rising groundwater table, the rise can be estimated by interpreting groundwater levels in the area. In general, groundwater

levels are depressed in younger mine spoil, but rise to a steady-state level over time as seepage in the spoil equilibrates with seepage in the previously existing ground.

Downward permeation of surface water will likely be restricted to approximately the upper 10 ft (3.0 m) because as surface water moves downward, it tends to carry fines with it, which ultimately clog the spoils and prevent further groundwater infiltration (Karem, 2005). With respect to impact on surface structures, the second mechanism is of greater concern because it occurs closer to the ground surface and can lead to larger amounts of differential settlement as seen in some case histories of mine spoil (Karem, 2005).

4.5 Summary

Mine spoil is a very heterogeneous material that is highly susceptible to large amounts of differential settlement. Because there are two primary mechanisms leading to this settlement, stress-induced crushing and hydrocompression, it can be difficult to accurately predict the amount of settlement that can be expected under future loading conditions. With the use of a common geophysical method, seismic surveying, the mine spoil subsurface profile can be determined and subsequently evaluated for settlement potential using the equations presented herein. For general purposes, mine spoil can be assumed to have an initial void ratio of approximately 0.68 if dry and 0.54 if wet, and stress-induced crushing index values (C_s) of 0.075 for dry mine spoil and 0.142 for wet mine spoil. Using the equations and methodology presented in this chapter, potential development sites can be screened for suitability based on settlement potential.

It should be noted that there are some differences between laboratory and field conditions. The stresses used to confine the samples for the laboratory testing were comparable to field stresses in the upper 15 ft (5.0 m) of mine spoil deposits, where most

of the deformation contributing to differential settlement occurs. The hydraulic gradients used in the lab to wet the samples were higher than typical hydraulic gradients encountered in the field. This was done to expedite laboratory testing, however the higher gradients are not believed to have a significant impact on the results. In addition, the material used in the lab was filtered on a 0.5-in. (1.3-cm) sieve so that the samples would be reasonably accommodated by the resonant column apparatus. In the field, boulders of a cubic yard (a cubic meter) or more may be present, and the material is much more heterogeneous. The presence of these boulders would tend to lessen volume change when compared to lab results, but increase differential settlement when compared to lab results.

4.5.1 Example problem

Given Figure 4.8, use the method presented in this chapter to determine the expected settlement due to an expected stress increase, $\Delta\sigma$, of 3000 psf (143.6 kPa). Assume that the settlement will be limited to the upper 15 ft (4.6 m) of the mine spoil and that all three layers are primarily sandstone.

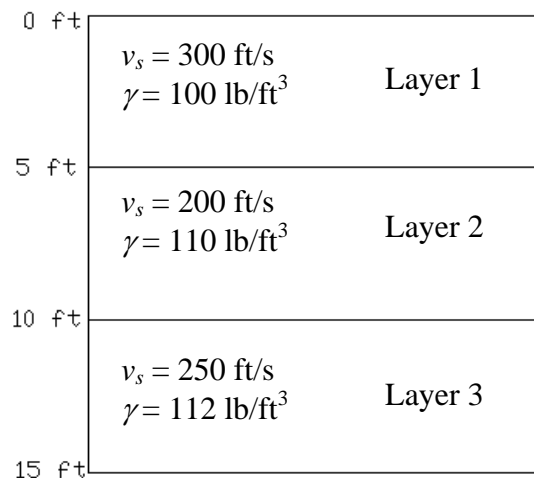


Figure 4.8. Example subsurface profile.

Step 1: Calculate the stress adjusted v_s, v_s' . Note subscripts 1, 2, and 3 represent layers 1, 2, and 3 respectively.

First calculate the vertical effective stress at the midpoint of each layer.

$$\sigma'_{v1} = 2.5 \text{ ft} \times (100 \text{ lb/ft}^3) = 250 \text{ lb/ft}^2$$

$$\sigma'_{v2} = [5 \text{ ft} \times (100 \text{ lb/ft}^3)] + [2.5 \text{ ft} \times (110 \text{ lb/ft}^3)] = 775 \text{ lb/ft}^2$$

$$\sigma'_{v3} = [5 \text{ ft} \times (100 \text{ lb/ft}^3)] + [5 \text{ ft} \times (110 \text{ lb/ft}^3)] + [2.5 \text{ ft} \times (112 \text{ lb/ft}^3)] = 1330 \text{ lb/ft}^2$$

Assume a ϕ' of 30 degrees and use equation 4.16 to calculate K_0 .

$$K_0 = 1 - \sin(\phi') = 1 - \sin(30) = 0.5$$

Then use Equation 4.15 to calculate the mean effective confining stress, σ'_o .

$$\sigma'_{o1} = \sigma'_{v1} \left(\frac{1 + 2K_0}{3} \right) = 250 \text{ lb/ft}^2 \left(\frac{1 + 2 \times 0.5}{3} \right) = 167 \text{ lb/ft}^2$$

$$\sigma'_{o2} = 517 \text{ lb/ft}^2$$

$$\sigma'_{o3} = 887 \text{ lb/ft}^2$$

Now use equation 4.14 to calculate v_s' .

$$v_{s1}' = \frac{v_s}{(\sigma'_o)^{0.25}} = \frac{300 \text{ ft/s}}{(1.16 \text{ psi})^{0.25}} = 289 \text{ ft/s/psi}^{0.25} > 275 \text{ ft/s/psi}^{0.25} \text{ therefore material is}$$

likely dry

$$v_{s2}' = 145 \text{ ft/s/psi}^{0.25} < 275 \text{ ft/s/psi}^{0.25} \text{ therefore material is likely wet}$$

$$v_{s3}' = 159 \text{ ft/s/psi}^{0.25} < 275 \text{ ft/s/psi}^{0.25} \text{ therefore material is likely wet}$$

Step 2: Calculate the expected settlement using Equations 4.17, 4.18, 4.19, and 4.20.

For our purposes we will assume an e_0 of 0.68 for the dry layers (layer 1) and 0.54 for the wet layers (layers 2 and 3). For dry layers (layer 1), $C_s = 0.075$. For wet layers (layers 2

and 3) $C_s = 0.142$. Note that for each layer we will calculate a wetted settlement and a dry settlement.

First calculate the settlement of wetted material using Equation 4.17:

$$S_{w1} = 0.0922H_o \log\left(\frac{\sigma_{f1}'}{\sigma_{v1}'}\right) = 0.0922(5\text{ft}) \log\left(\frac{3250\text{psf}}{250\text{psf}}\right) = 0.51\text{ ft} = 6.2\text{ in}$$

$$S_{w2} = 3.8\text{ in}$$

$$S_{w3} = 2.8\text{ in}$$

Next calculate the settlement of dry material using Equation 4.18:

For sandstone, $\varepsilon = 0.07$

$$S_{d1} = H_o \left[0.0446 \log\left(\frac{\sigma_{f1}'}{\sigma_{v1}'}\right) + \varepsilon \right] = (5\text{ft}) \left[0.0446 \log\left(\frac{3250\text{psf}}{250\text{psf}}\right) + 0.07 \right] = 0.60\text{ ft} = 7.2\text{ in}$$

$$S_{d2} = 6.0\text{ in}$$

$$S_{d3} = 5.6\text{ in}$$

Now calculate the weighted total settlement of each layer using equation 4.20 for layer 1 (dry) and 4.19 for layers 2 and 3 (wet):

$$S_1 = 0.28S_{w1} + 0.72S_{d1} = 0.28(6.2\text{ in}) + 0.72(7.2\text{ in}) = 6.9\text{ in}$$

$$S_2 = 0.67S_{w2} + 0.33S_{d2} = 0.67(3.8\text{ in}) + 0.33(6.0\text{ in}) = 4.5\text{ in}$$

$$S_3 = 0.67S_{w3} + 0.33S_{d3} = 0.67(2.8\text{ in}) + 0.33(5.6\text{ in}) = 3.7\text{ in}$$

To find the total settlement of the mine spoil sum the layer settlement values:

$$S = S_1 + S_2 + S_3 = 6.9\text{ in} + 4.5\text{ in} + 3.7\text{ in} = 15.1\text{ in}$$

CHAPTER FIVE

EFFECT OF COMPACTION EFFORT AND MOISTURE CONTENT ON SETTLEMENT POTENTIAL

5.1 Introduction

In the field, compaction effort can vary; therefore it is important that multiple compaction efforts be evaluated for their effect on settlement potential. ASTM D698 and ASTM D1557 (standard Proctor test and modified Proctor test) are the two most commonly used laboratory tests for generating compaction curves and these two were used to represent the effect of compaction effort on settlement potential of the mine spoil.

In addition to compaction effort, moisture content was expected to have an effect on the settlement potential of the mine spoil. Because hydrocompression is a primary cause of harmful differential settlement in mine spoil, it was predicted that samples with moisture contents dry of optimum would exhibit increased volume reduction due to hydrocompression when wetted. In previous studies and field observations, mine spoil that had already undergone hydrocompression did not show appreciable settlement with additional wetting (Karem, 2005). Therefore it was predicted that samples wet of optimum would undergo hydrocompression immediately and then no longer be susceptible.

5.2 Lab Procedure

The material used for the testing consisted of a blend of material recovered from six different locations. The blended material was filtered on a No. 4 (4.75 mm) sieve and the fraction passing the sieve was compacted per ASTM D698 and ASTM D1557 (standard and modified Proctor tests respectively). Due to limited available quantities of

materials, the soil locations were mixed together to form two soils, rather than six. The soil mixtures were chosen based on similar mineralogical properties. Locations 1, 2, and 6 were combined, making a primarily siltstone with some mudstone soil mixture (Blend #1). Locations 3, 4, and 5 were combined making a primarily sandstone mixture (Blend #2). The mixtures were compacted per ASTM D698 for standard Proctor and ASTM D1557 for modified Proctor. The samples were removed from the Proctor mold using a hand press, making samples that were 4.6 in. (12 cm) in height with a 4.0 in. (10 cm) diameter. After compaction the samples were placed in a triaxial cell that was attached to a pressure board (see Figures 5.1 and 5.3). The samples were placed in latex membranes with filter paper and a porous stone on each end (see Figure 5.1). The top of the sample had a cap attached to the latex membrane using an O-ring (see Figure 5.2). The bottom of the sample sat on the base of the triaxial cell and the latex membrane was attached using an O-ring (see Figure 5.1).



Figure 5.1. Sample setup showing triaxial cell and sample close-up.



Figure 5.2. Sample end cap and vacuum line.



Figure 5.3. Pressure board.

Before sealing the triaxial cell, a pore vacuum of 6.0 psi (41 kPa) was applied to both ends of the sample and the height and three diameter measurements were recorded. The diameter measurements were taken at the bottom, top, and middle of each sample. After recording the measurements, the triaxial cell was sealed by placing the outer casing over the sample and tightening the screw rods. A cell pressure of 6.0 psi (41 kPa) of air was applied to the sample and the vacuum pressure was turned off. The influent chamber was filled with water, and a vacuum of 6.0 psi (41 kPa) was applied to the top of the specimen. The specimen was then wetted from the bottom up to impose a pore pressure gradient of 6.0 psi (41 kPa), which is equivalent to 13.8 ft (4.21 m) of head. No vacuum was applied at the base of the sample, giving it a vacuum pressure of 0 psi (0 kPa) and an average vacuum pressure in the sample of 3.0 psi (21 kPa). Thus, the average effective stress in the specimen was 9.0 psi (62 kPa) [6.0 psi (41 kPa) of cell pressure plus 3.0 psi (21 kPa) of negative pore pressure].

The specimen was wetted from the bottom up to assist in dislodging and removing air bubbles in the system. The sample was left in the triaxial cell for 24 hours. After 24 hours the confining pressure was turned off and the triaxial case was removed. Vacuum pressure of 6.0 psi (41 kPa) was applied to both ends of the specimen and the measurements were recorded again. The sample was left in the chamber for 24 hours due to the very slow migration of water through the sample. After measurements were recorded the sample was removed, weighed, and oven dried for 24 hours and then re-weighed to determine the degree of saturation and moisture content post-wetting.

The above mentioned procedure was used for the majority of the specimens; however a few of the earlier specimens were not wetted in this manner. The specimens

were prepared by placing them in a latex membrane and then setting the sample on end on a porous stone with filter paper between the porous stone and sample. The bottom of the sample was placed in a pan with standing water, with a slight overhang of the latex membrane to create suction to the bottom of the pan. This procedure was based on the procedure for freezing and thawing soil-cement mixtures to encourage water absorption as described in ASTM D560, “Standard Test Methods for Freezing and Thawing Compacted Soil-Cement Mixtures.” Filter paper and a porous stone were placed on the top of the specimen with an end cap attached to the latex membrane with an O-ring. A 6.0 psi (41 kPa) vacuum was applied to the top of the specimen and water was drawn up through the specimen similar to the previous procedure. This procedure was abandoned because it was difficult to eliminate leaks.

5.3 Results

Volumetric strain was computed as change in volume divided by the initial volume and is given as a percentage. A negative strain value indicates a decrease in volume (contraction) while a positive strain value indicates an increase in volume (dilation).

5.3.1 Effect of compaction effort on relative change in volume

The effect of compaction effort was evaluated to determine if there was a correlation between compaction effort and settlement potential. Generally speaking, samples that were compacted with a higher compaction effort (modified Proctor) dilated slightly after wetting, and samples compacted with a lower compaction effort (standard Proctor) contracted slightly after wetting.

Within the soil matrix, two volume change mechanisms appear to exist. The first is hydrocompression (i.e. a sudden loss in volume due to wetting), where the individual soil particle edges soften at points of contact when wetted and therefore are easily crushed due to confining stresses. For the relatively loose samples, in particular the standard Proctor samples, this is the dominant mechanism. The second mechanism is caused by swelling due to expansive clay particles in the soil matrix. Clay swells when wetted due to its desire to adsorb water into its double layer. For the denser samples, in particular the modified Proctor samples, enough particle crushing occurred prior to wetting, lessening and possibly eliminating the potential for hydrocompression. For these denser samples the tendency for the clay particles to swell overcame the tendency of the shale particles to hydrocompress, creating a net effect of slight volume increase under the given confining stress. If a higher confining stress had been used, the denser samples would have most likely lost volume due to hydrocompression or not shown any appreciable volume change as the confining stress would have essentially overpowered the swell forces of the clay particles.

For the standard Proctor samples, the samples wet of optimum generally saw more volume change than those dry of optimum. This was not expected as the original hypothesis was that if the samples were dry of optimum they would be more prone to hydrocompression. However this can be explained by looking at the unit weights. The samples wet of optimum did not compact very well and therefore were less dense. The reason this phenomenon was not observed in the modified Proctor samples is likely due to the fact that the modified effort was great enough to adequately reduce the void spaces. Figure 5.4 shows the comparison of standard and modified Proctor dry unit weights for

both soil types. Looking at these curves, it is easily seen that the L1/2/6 samples achieved much higher dry unit weights at much lower moisture contents.

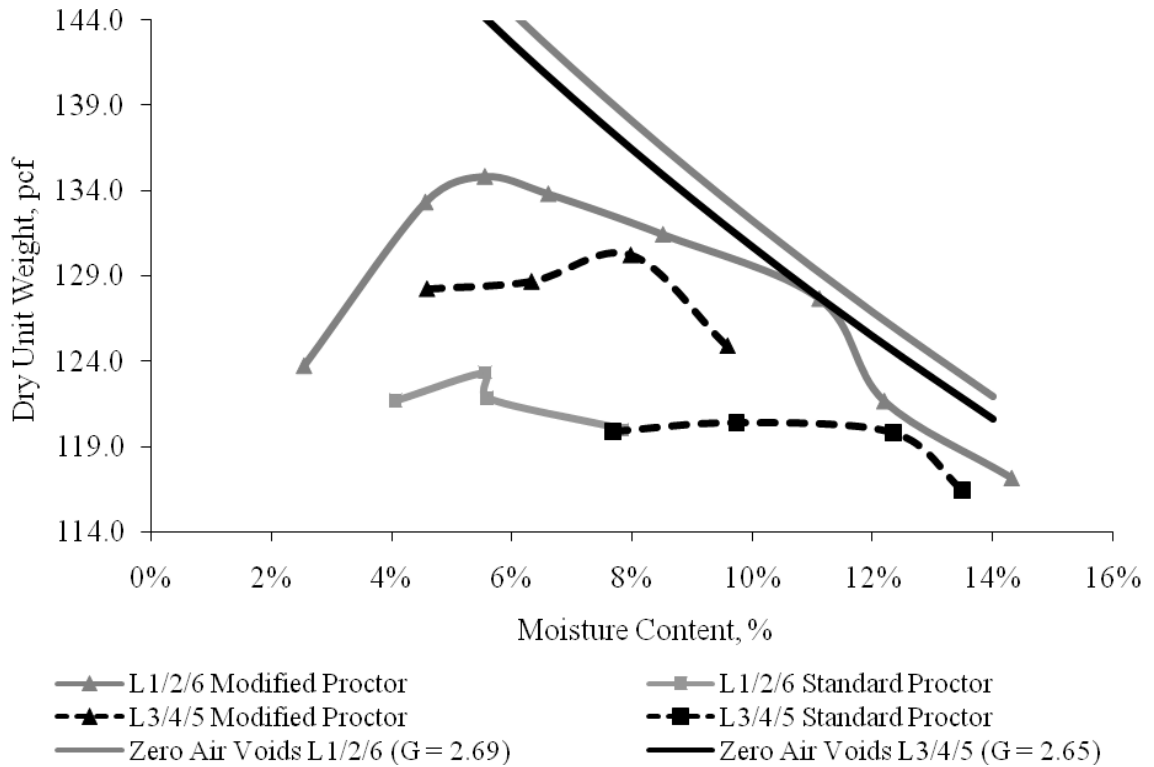


Figure 5.4. Compaction curves for soil L1/2/6 and L3/4/5.

On average, the L1/2/6 modified Proctor samples showed less volume change than the other specimens, which is consistent with the theory that higher initial unit weight corresponds to decreased settlement potential. This is also illustrated in Figure 5.5 which compares volumetric strain to the dry unit weight. For the most part, samples with higher initial unit weight showed less volume change than those with lower initial unit weight, and nearly all of the standard proctor specimens had negative volume change (contraction).

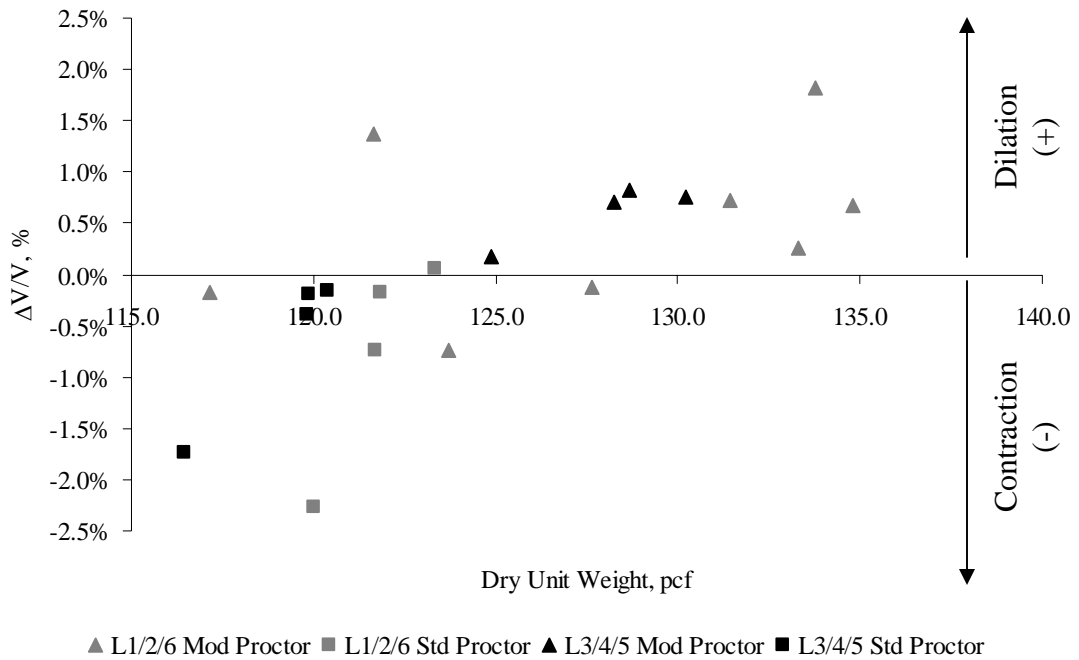


Figure 5.5. Volumetric strain versus dry unit weight.

5.3.2 Effect of moisture content on relative change in volume

It was originally hypothesized that samples dry of optimum moisture content would be more prone to hydrocompression than samples wet of optimum moisture content. However the lab data show little correlation between initial moisture content and settlement potential, as shown in Figure 5.6.

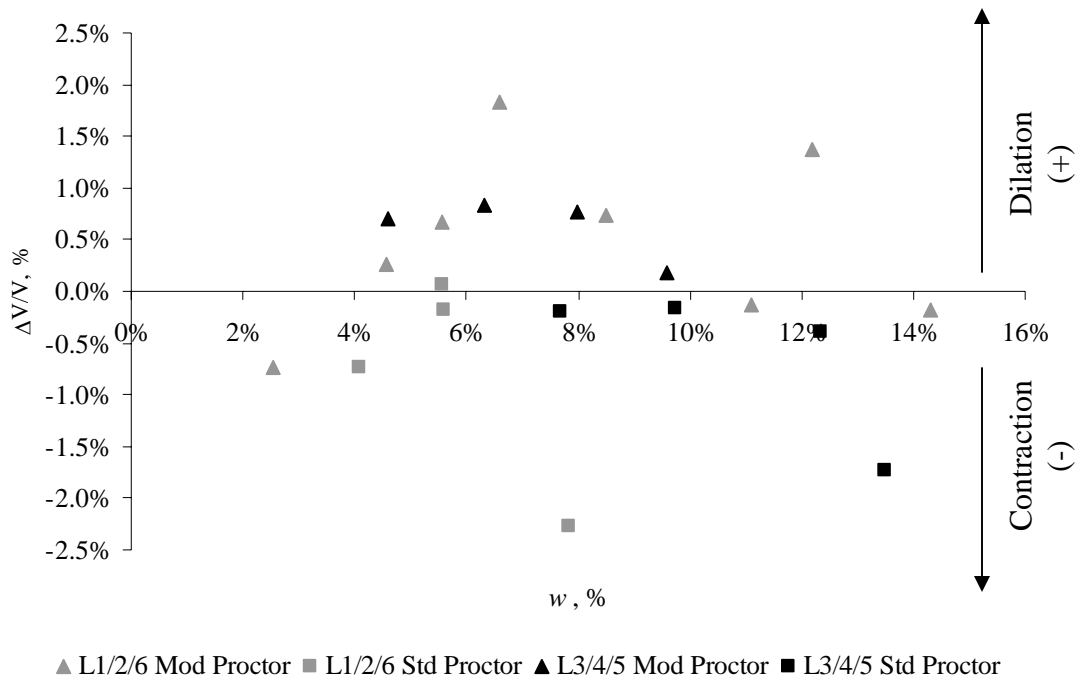


Figure 5.6. Volumetric strain versus moisture content.

5.3.3 Effect of dry unit weight and initial void ratio on relative change in volume.

Dry unit weight and volumetric strain data was compared for both the compaction testing phase and the shear wave testing phase. The samples used in Chapter 4 of this text were not compacted and therefore had significantly lower dry unit weights than the compacted samples. However they showed a similar trend to what was seen in the compaction samples, as illustrated in Figure 5.7, where the uncompact specimens are combined with the compacted specimens from Figure 5.5.

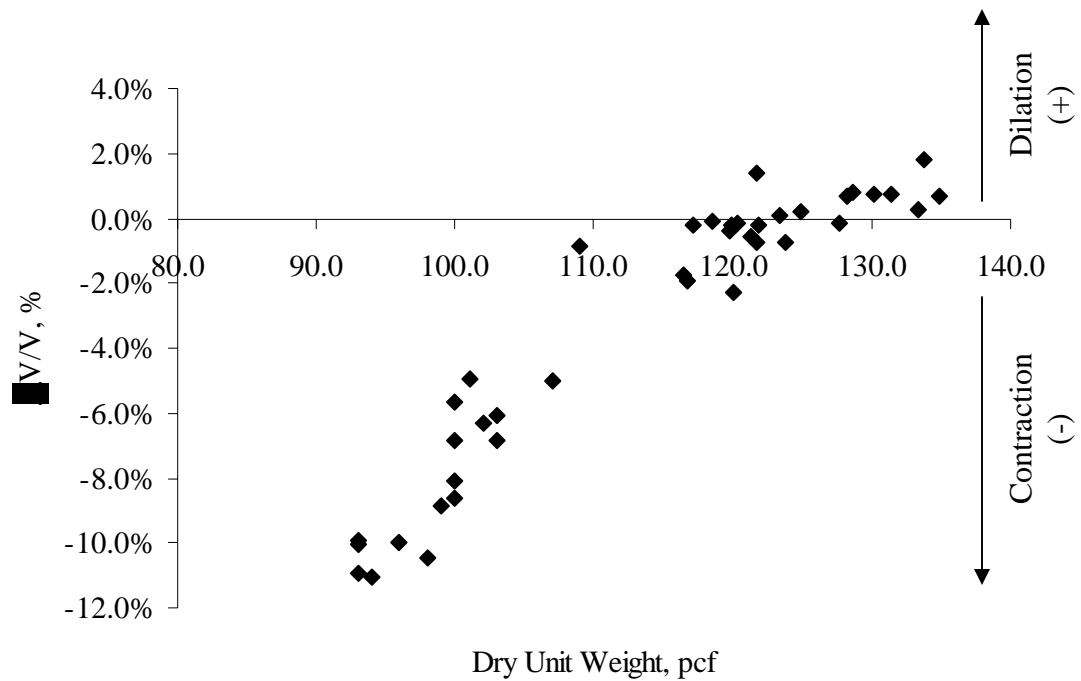


Figure 5.7. Volumetric strain versus dry unit weight.

Reviewing Figure 5.7, a clear relationship between dry unit weight and volume change can be observed. For unit weights above 120 pcf (18.8 kN/m³) volumetric strain is nearly zero, however for dry unit weights below this threshold value, volumetric strains dramatically increase, going to greater than 10% in a few cases.

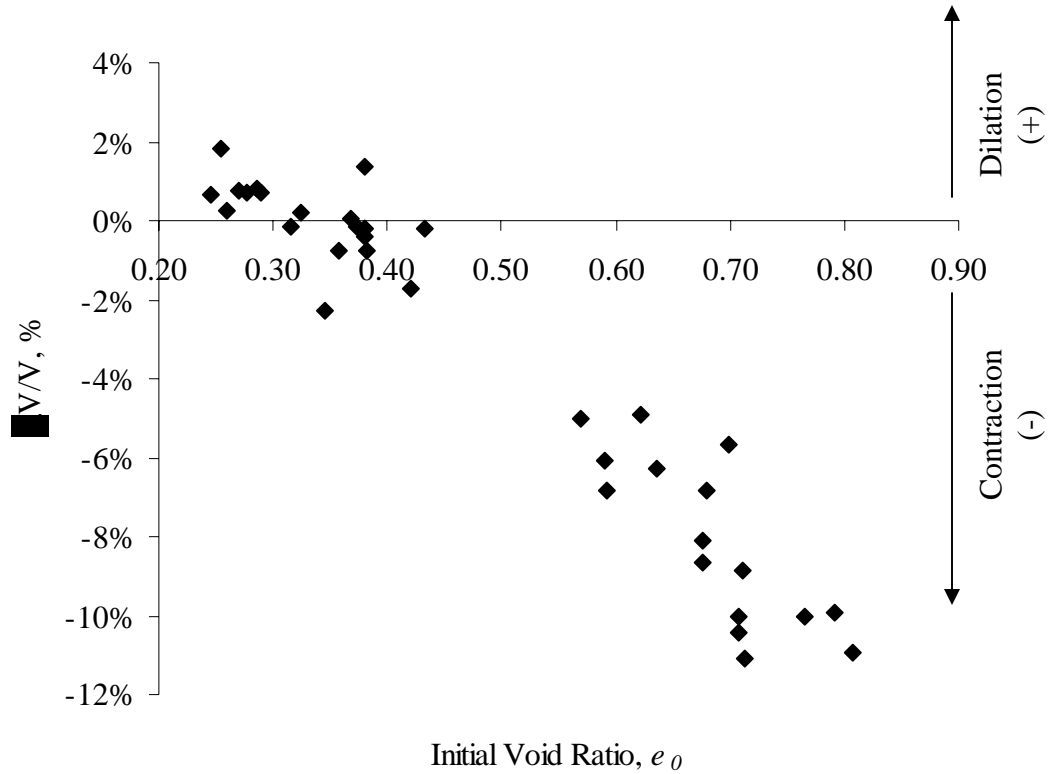


Figure 5.8. Volumetric strain versus initial void ratio.

Evaluating the data from Figure 5.8 in terms of initial void ratio, a relationship between initial void ratio, e_0 (void ratio before saturation, but after sample preparation or compaction), and volumetric strain can be observed (Figure 5.8). It is apparent that void ratios less than about 0.45 show negligible volumetric strain, whereas void ratios greater than 0.50 show substantial volumetric strain and settlement potential. Also, in general it is apparent that void ratios greater than 0.50 will show compressive behavior when wetted, while void ratios less than or equal to 0.45 will show dilative behavior.

A trend line was fitted to the data shown in Figures 5.7 and 5.8 and the following empirical quadratic relationships were developed:

$$\frac{\Delta V}{V} = -7 \times 10^{-5} \gamma_d^2 + 0.0193 \gamma_d - 1.2786 \quad (R^2 = 0.95) \quad (5.1)$$

$$\frac{\Delta V}{V} = -0.1921e_0^2 - 0.0308e_0 + 0.0319 \quad (R^2 = 0.94) \quad (5.2)$$

5.4 Summary

While it was originally hypothesized that initial moisture content would drive the settlement/volume change potential of the compacted mine spoils, the lab data showed that dry unit weight was the driving factor. Samples that were compacted with higher effort and achieved higher dry unit weights showed less volumetric strain than those with lower compaction effort and dry unit weights. In addition, even the samples compacted with the lower compaction effort (standard Proctor) showed small volume change overall, which indicates that even a relatively small compaction effort is very beneficial for reducing settlement potential. For example, if a 10.0-ft. (3.05 m) thick layer of mine spoil composed of L1/2/6 material at 8% moisture content was compacted using standard effort, it could be expected to settle 2.7-in. (6.8 cm), and that would be the worst case scenario from the lab data acquired. If one were to compact that same 10.0-ft (3.05 m) layer of L1/2/6 soil at optimum moisture content (5.56%) settlement of only 0.08-in. (0.2 cm) would be expected based on the lab data. If the same 10.0-ft (3.05 m) layer of mine spoil is not compacted, assuming an initial void ratio of 0.70, settlement of 6.8-in. (17 cm) would be expected. Even if the initial void ratio is 0.57, the 10.0-ft (3.05 m) layer of uncompacted mine spoil would be expected to settle 6.0-in (15 cm). This indicates that mine spoil that is properly compacted with at least standard Proctor effort should be expected to show little settlement in the field. In addition, mine spoil similar to that tested should show little to no volume change if compacted to a dry unit weight of 120 pcf (18.8 kN/m³) or greater or to a void ratio of less than 0.50.

CHAPTER SIX

SUMMARY AND RECOMMENDATIONS

6.1 Research Summary

The goal of this research was to determine the effect of stress conditions, wetting, and compaction effort on the susceptibility of mine spoil to settle. Representative mine spoil samples were recovered from the Gateway Business Park near Jenkins, Kentucky, and laboratory tests were performed on reconstituted specimens of this material. As a result of this study, two main settlement-inducing mechanisms were observed. The first mechanism is crushing due to an increase in the confining stress of the specimen as angular particles crush at points of contact. A second, more severe mechanism is hydrocompression, where the mine spoil undergoes a sudden and dramatic loss in volume when wetted. On average, vertical strains associated with hydrocompression are around 10%.

Relationships were developed between confining stress, wetting, and shear wave velocity for the mine spoil. These relationships could be used to screen potential sites for development. Several equations were developed to predict the amount of settlement mine spoil would undergo based on three quantities: expected load placed on the mine spoil, in situ shear wave velocity, and spoil mineralogy (i.e. sandstone, siltstone, or mudstone). In addition, a correlation between shear wave velocity and probability of the mine spoil already being wet was found. An overburden-corrected shear wave velocity, v_s' , of greater than $275 \text{ ft/s/psi}^{0.25}$ indicated dry mine spoil, while a v_s' of less than $275 \text{ ft/s/psi}^{0.25}$ indicated wet mine spoil. This is important because mine spoil that has already been wet

has likely undergone hydrocompression and is therefore not susceptible to further hydrocompression induced settlement.

These results indicate that shear wave velocity can be used to estimate the total settlement of a mine spoil subsurface profile. In general, shear wave velocity of mine spoil specimens decreased after wetting. In typical geotechnical applications, a higher shear wave velocity is desirable because it generally means the material is denser and therefore stronger. For the case of mine spoil however, a lower shear wave velocity is actually desirable because it means the material has likely already hydrocompressed and will therefore not be susceptible to moisture induced settlement in the future.

Based on these observations, a method to predict settlement potential was developed. Using this approach, settlement potential (S) can be estimated using the following equations:

$$\text{Wet mine spoil } (v_s' < 275 \text{ ft/s/psi}^{0.25}): S = 0.67S_w + 0.33S_d. \quad (4.19)$$

$$\text{Dry mine spoil } (v_s' > 275 \text{ ft/s/psi}^{0.25}): S = 0.28S_w + 0.72S_d. \quad (4.20)$$

The settlement of wetted material (S_w) and dry material (S_d) can be estimated using the following equations:

$$S_w = 0.0922H_o \log\left(\frac{\sigma_f'}{\sigma_0'}\right). \quad (4.17)$$

$$S_d = H_o \left[0.0446 \log\left(\frac{\sigma_f'}{\sigma_0'}\right) + \varepsilon \right]. \quad (4.18)$$

Equations 4.17 and 4.18 illustrate the two mechanisms. The first mechanism, stress-induced crushing, is quantified by the logarithm term in the two equations. The second mechanism, settlement due to wetting, is quantified by the strain term, ε . Note that the wet settlement equation does not have a strain term; this is because once mine spoil has

undergone hydrocompression (as in situ wet mine spoil would) it is no longer susceptible to further moisture induced settlement. As indicated by these two equations, the first mechanism should be expected in material that has been previously wetted, while both mechanisms should be expected in material that has never been wetted.

With regard to compaction effort and moisture content, it was found that initial moisture content did not have a significant effect on the settlement potential. In other words, samples that were initially wet or dry of optimum moisture content did not exhibit any pattern with regards to volume change caused by wetting. However, correlations were made based on dry unit weight and initial void ratio of the mine spoil after compaction with volume change/settlement potential. It was found that samples that were compacted to at least 120 pcf (18.8 kN/m³) or a post-compaction void ratio of 0.45 would experience little to no volume change. This information could be very useful to engineers, developers, and contractors for construction quality assurance programs. Essentially what this research has shown is that if the mine spoil is compacted to a dry unit weight of at least 120 pcf (18.8 kN/m³), regardless of compaction effort, the mine spoil would not be expected to settle significantly due to water infiltration.

6.2 Future Research

This research was performed using laboratory specimens under highly controlled circumstances; therefore field tests should be performed to validate the conclusions presented herein. It is recommended that shear wave velocity testing be performed at existing mine spoil sites along with borings to validate the shear wave velocity correlations developed as part of this research.

With regard to compaction, test pads would be a good way to validate the conclusions regarding dry unit weight. Test pads could be constructed and compacted to different dry unit weights and then wetted to field test the conclusions derived in Chapter 5 regarding dry unit weight and void ratio.

In addition to field testing the methods presented in this paper, it should be noted that the material used for the testing came from only one site in Eastern Kentucky. To add to the value of this research, materials from more sites should be used for testing.

APPENDIX A

EFFECT OF COMPACTION ON SETTLEMENT POTENTIAL RAW DATA

Table A.1. L1/2/6 and L6 compaction results summary.

Sample ID	γ_d (lb/ft ³)	w (%)	$\Delta V/V$ (%)	TC?
Mod 1%	123.7	2.6%	-0.74%	
Mod 5%	133.3	4.6%	0.26%	X
Mod Opt	134.8	5.6%	0.68%	X
Mod 7%	133.8	6.6%	1.82%	
Mod 9%	131.4	8.5%	0.73%	X
Mod 11%	127.6	11.1%	-0.13%	X
Mod 13%	121.7	12.2%	1.38%	X
Mod 15%	117.1	14.3%	-0.18%	
Std 6%	121.8	5.6%	-0.18%	X
Std 8%	120.0	7.8%	-2.27%	X
Std 4%	121.7	4.1%	-0.74%	X
Std Opt	123.3	5.6%	0.07%	X
Std L6 11%	121.2	9.1%	-0.58%	
Std L6 13%	118.5	13.6%	-0.08%	
Std L6 15%	116.7	13.7%	-1.93%	
Std L6 17%	109.0	18.4%	-0.89%	

Table A.2. L3/4/5 compaction results summary.

Sample ID	γ_d (lb/ft ³)	w (%)	$\Delta V/V$ (%)	TC?
Mod 4%	128.2	4.6%	0.71%	X
Mod 6%	128.7	6.3%	0.83%	X
Mod 8%	130.2	8.0%	0.76%	X
Mod 10%	124.9	9.6%	0.18%	X
Std 8%	119.9	7.7%	-0.20%	X
Std 10%	120.4	9.7%	-0.16%	X
Std 12%	119.8	12.3%	-0.40%	X
Std 14%	116.4	13.5%	-1.74%	X

NOTE: TC indicates sample was wetted using the triaxial cell method.

Positive $\Delta V/V$ indicates dilation; negative $\Delta V/V$ indicates contraction.

Table A.3. Dry density and void ratio summary.

$\Delta V/V$ (%)	e_0	γ_d (lb/ft ³)	$\Delta V/V$ (%)	e_0	γ_d (lb/ft ³)
-5.65%	0.70	100.0	0.18%	0.32	124.9
-8.86%	0.71	99.0	-0.20%	0.38	119.9
-8.64%	0.68	100.0	0.76%	0.27	130.2
-8.09%	0.68	100.0	-1.74%	0.42	116.4
-10.44%	0.71	98.0	0.83%	0.29	128.7
-10.04%	0.76	93.0	0.71%	0.29	128.2
-10.01%	0.71	96.0	-0.74%	0.36	123.7
-4.92%	0.62	101.0	0.26%	0.26	133.3
-6.06%	0.59	103.0	0.68%	0.25	134.8
-6.84%	0.59	103.0	1.82%	0.25	133.8
-6.84%	0.68	100.0	0.73%	0.28	131.4
-6.30%	0.64	102.0	-0.13%	0.31	127.6
-5.04%	0.57	107.0	1.38%	0.38	121.7
-9.94%	0.79	93.0	-0.18%	0.43	117.1
-10.95%	0.81	93.0	-0.18%	0.38	121.8
-11.07%	0.71	94.0	-2.27%	0.35	120.0
-0.16%	0.37	120.4	-0.74%	0.38	121.7
-0.40%	0.38	119.8	0.07%	0.37	123.3

REFERENCES

- Das, B. M. (2002). *Principles of Geotechnical Engineering, 5th Edition*. Pacific Grove, CA: Brooks/Cole.
- Ebelhar, R. J. (1976). *Evaluation of a technique for estimating the shear strength of a mine spoil material*. Ph.D. Dissertation. Lexington, KY: University of Kentucky.
- Hardin, B. O., and Drnevich, V. (1972). Shear Modulus and Damping in Soils: Design Equations and Curves. *Journal of the Soil Mechanics and Foundations Division, Proceedings of the American Society of Civil Engineers*, Vol. 98, No. SM7, July 1972, 667-692.
- Kalinski, M. E., and Thummaluru, M. S. R. (2005). A New Free-Free Resonant Column Device for Measurement of G_{max} and D_{min} at Higher Confining Stresses. *Geotechnical Testing Journal*, Vol. 28, No. 2, 180-187.
- Karem, W. A. (2005). *Development of a predictive model to evaluate mine spoil fills for industrial development*. Ph.D. Dissertation. Lexington, KY: University of Kentucky.
- Karem, W. A., Kalinski, M. E., and Hancher, D. E. (2007). Settlement of mine spoil fill from water infiltration: a case study in Eastern Kentucky. *Journal of Performance of Constructed Facilities*, 21(5), 345-350.
- Kentucky Cabinet for Economic Development (2008). *Gateway Regional Business Park*. Retrieved January 16, 2008, from <http://www.thinkkentucky.com/>.
- Krebs, R. D., and Zipper, C. E. (2007). *Foundations for Housing on Reclaimed Mine Lands*. Retrieved February 13, 2008, from <http://www.ext.vt.edu/pubs/mines/460-115/460-115.html>

Rosentiel, A. (2006). *Mine Spoil Analysis*. Master's Project. Lexington, KY: University of Kentucky.

Seed, H. B., Wong, R. T., Idriss, I. M., and Tokimatsu, K. (1986). Moduli and Damping Factors for Dynamic Analyses of Cohesionless Soils. *Journal of Geotechnical Engineering*, American Society of Civil Engineers, Vol. 112, No. 11, 1016-1032.

Skelly, and Loy. (1979). *Illustrated Surface Mining Methods*. New York: McGraw Hill, Inc.

VITA

Lauren M. Little was born in Fairbanks, Alaska on November 5, 1984. She attended the University of Alaska Fairbanks where she received a Bachelors of Science degree in 2006 and graduated Cum Laude.